



Biomass and nutrient dynamics of major green tides in Ireland: Implications for biomonitoring

Ricardo Bermejo^{a,b,*}, Nessa Golden^a, Elena Schrofner^{a,c}, Kay Knöller^d, Owen Fenton^e, Ester Serrão^c, Liam Morrison^{a,**}

^a Earth and Ocean Sciences, School of Natural Sciences and Ryan Institute, National University of Ireland, Galway H91 TK33, Ireland

^b Department of Biology, Faculty of Marine and Environmental Sciences, University of Cadiz, E11510 Puerto Real, Spain

^c Center of Marine Sciences (CCMAR), CIMAR Laboratório Associado, Campus de Gambelas, Universidade do Algarve, 8005-139 Faro, Portugal

^d Department of Catchment Hydrology, Helmholtz-Centre for Environmental Research, UFZ Theodor-Lieser-Straße 4, D-06120 Halle, Germany

^e Teagasc, Johnstown Castle, Co, Wexford, Ireland

ARTICLE INFO

Keywords:

Green tide
Nitrogen
Phosphorus
Ulva
Tissue nutrient content
Nitrogen isotope ratio

ABSTRACT

The control of macroalgal bloom development is central for protecting estuarine ecosystems. The identification of the nutrients limiting the development of macroalgal blooms, and their most likely sources is crucial for management strategies. Three Irish estuaries (Argideen, Clonakilty and Tolka) affected by green tides were monitored from June 2016 to August 2017. During each sampling occasion, biomass abundances, tissue N and P contents, and $\delta^{15}\text{N}$ were determined for tubular and laminar morphologies of *Ulva*. All estuaries showed maximum biomass during summer and minimum during winter. Tissue nutrient contents revealed P rather than N limitation. The $\delta^{15}\text{N}$ during the peak bloom indicated agriculture as the most likely source of nitrogen in the Argideen and Clonakilty, and urban wastewaters in the Tolka. No differences in the $\delta^{15}\text{N}$, and the tissue nutrients content were observed between morphologies. The period between May and July is most suitable for bio-assessment of green tides.

1. Introduction

Estuaries are relatively small water bodies with low rates of water renewal, and are the first recipients of pollutants via rivers in the land to sea pathway. This combination makes these areas especially susceptible to pollution including nutrient over enrichment and the associated development of macroalgal blooms (Teichberg et al., 2010; Valiela et al., 1997). Macroalgal blooms or seaweed tides consist of the accumulation of huge masses of fast-growing opportunistic species, mainly Ulvoids. Although these blooms are not toxic by themselves, these alter the structure and functioning of estuarine ecosystems, limiting the services they provide (Corzo et al., 2009; Krause-Jensen et al., 2008; Lenzi et al., 2012). The accumulation of large amounts of seaweed biomass and thick canopies of seaweeds physically obliterate other coastal life (Hauxwell et al., 2001) and may prevent the use of these waters (e.g. hampering navigation, clogging of pipes; fouling fishing lines and nets; Critchley et al., 1986; Gao et al., 2010; Smetacek and Zingone, 2013). Moreover, the subsequent decay of large amounts of seaweed biomass produces

unpleasant odours (Teichberg et al., 2010; Wan et al., 2017), anoxic conditions that lead to fish and shellfish deaths (Baden et al., 1990; Worm et al., 1999), and can favour the proliferation of opportunistic plagues such as chironomic flies (Fletcher, 1996).

The most recent assessment of the ecological status of Irish water bodies in the context of the Water Framework Directive (WFD, 2000/60/EC) for the period 2013–2018 (O'Boyle et al., 2019) revealed that the 62% of the 79 transitional water bodies (i.e. estuaries and coastal lagoons) investigated showed an ecological status of moderate or worse. A quarter of transitional and coastal waters failed the environmental quality standard and assessment criteria for DIN, and it was reported that nitrogen and phosphorus loads started to increase (16% and 31% respectively, since 2012–2014) after many years of reductions (O'Boyle et al., 2019). The most problematic areas were located in the south and south east of the country in regions of intensive agriculture, and along the east coast in close proximity to Dublin City (Trodd and O'Boyle, 2021). One of the indices considered to determine the ecological status of transitional waters in Ireland is based on the assessment of macroalgal

* Correspondence to: R. Bermejo, Department of Biology, Faculty of Marine and Environmental Sciences, University of Cadiz, E11510 Puerto Real, Spain.

** Corresponding author.

E-mail addresses: ricardo.bermejo@uca.es (R. Bermejo), liam.morrison@nuigalway.ie (L. Morrison).

bloom severity (Scanlan et al., 2007), thus the control of macroalgal blooms in Irish estuaries is key to compliance with the requirements of the European WFD.

Species of *Ulva*, including the former genus *Enteromorpha*, are among the main opportunistic macroalgae responsible for the occurrence of macroalgal blooms in estuarine environments (Hernandez et al., 1997; Malta et al., 1999; Valiela et al., 1997). These species exhibit a simple morphology, consisting either of a monostromatic tubular thallus (formerly *Enteromorpha* genus) or a distromatic laminar thallus (Hayden et al., 2003). Several studies highlighted the morphological diversity of macroalgal blooms containing tubular and laminar morphologies of *Ulva* (e.g., Fong et al., 1996; Hull, 1987; Jeffrey et al., 1995). Although *Ulva* species are phylogenetically close and many of them usually thrive in similar environments (Hayden et al., 2003; Valiela et al., 1997), these species are able to coexist and display temporal and spatial successions indicating different environmental requirements or unequal resistance to stressors (Bermejo et al., 2019b; Fong et al., 1996; Yabe et al., 2009). Morphologies have been frequently used to predict productivity and other ecological attributes (e.g., grazing resistance, competitive abilities, reproductive effort; Littler et al., 1983). Morphological diversity can lead to varying ecological performance and niche differentiation. In the case of *Ulva*, tubular morphologies are able to remain attached to the substrate, while the laminar ones are usually free floating as a consequence of the interaction of their morphology with environmental hydrodynamic features (Bermejo et al., 2019b; Salomonsen et al., 1997; Schories and Reise, 1993). This difference can play an important role in the response to stress or resource exploitation resulting in a different biological performance. For example, the burial of the basal part of tubular morphologies may provide access to nutrients from porewaters, which would not be available to laminar morphologies (Bermejo et al., 2019b; Robertson and Savage, 2018). It is expected that the tubular morphologies show a greater vertical heterogeneity in ecophysiological variables (e.g. tissue nutrient content, photosynthetic performance, pigment concentration) when occurring in dense aggregations than the laminar forms, as result of the more stable vertical structure of the tubular canopy due to anchorage to the substrate (Malta et al., 2003; Vergara et al., 1998). Moreover, because of the more complex morphology of tubular forms, they are likely more prone to contamination from the sediment than the laminar forms (e.g., Villares et al., 2001). All these factors could increase uncertainty in bioassessment and should be considered when designing sampling strategies."

As with other primary producers, the principal environmental drivers controlling the development of opportunistic bloom forming species are light, temperature and nutrients (Lotze et al., 1999, 2001; Valiela et al., 1997). In cold temperate estuaries, primary producers growth is usually limited by light and temperature during the winter, and by nutrients during spring and summer (Bermejo et al., 2019b; McGovern et al., 2019; Wang et al., 2012). Nitrogen and phosphorus are considered the main limiting nutrients for freshwater and coastal ecosystems (Howarth et al., 2000; Lapointe, 1987). In the case of temperate coastal and estuarine areas under limited human disturbances, N limitation rather than P limitation may control primary production during spring and summer, determining the composition of macrophyte communities (Howarth et al., 2000; Sfriso et al., 1987; Valiela et al., 1997). Although P loadings have also increased with the development of agriculture and the increase of human population, this increase has been proportionally smaller when compare with the increase in N loadings, producing a global shift in N:P ratio of nutrient loads, which might affect nutrient limitation patterns (Glibert, 2017; Lu and Tian, 2017; Teichberg et al., 2010). Changes in nutrient limitation patterns or relative nutrient enrichment can produce shifts in the composition of bloom forming species (e.g. from algae to nitrogen fixed cyanobacteria or vice versa; Glibert, 2017; Ní Longphuirt et al., 2015), and affect the spatial distribution patterns of eutrophication (Boesch, 2019; Ní Longphuirt et al., 2015). For instance, in areas close to the Rhine and Elba rivers, more rapid and substantial reductions in P than in N lead to a reduction in

primary productivity near the river mouths, which favoured the exportation of N up the coast, increasing the area affected by eutrophication until a reduction in N loads was also achieved (Boesch, 2019).

The concentration of dissolved nutrients in water provide limited information about their relative and quantitative importance in limiting growth and productivity in aquatic ecosystems, as this observed concentration is dependent on nutrient uptake by primary producers. In addition, it can also be very transient and variable depending on the hydrological conditions and the nature of nutrient sources, especially in complex systems such as estuaries (Bermejo et al., 2019b; Costanzo et al., 2000; Valiela et al., 1997). By contrast, the internal nutrient pool found in primary producers and their ratios provide more relevant information about the role of certain nutrients as limiting factors for the development of macroalgal blooms (Björnsäter and Wheeler, 1990; Fong et al., 1998; Lyngby et al., 1999). Several studies have been carried out in the laboratory to determine the critical and subsistence quota for N and P in *Ulva* spp. (Hernández et al., 2008; Pedersen and Borum, 1996; Villares and Carballeira, 2004). The critical quota is the minimum tissue nutrient content necessary to support unrestrained growth by the lack of nutrients, and the subsistence quota is the lowest nutrient tissue content that allows growth (Pedersen and Borum, 1996; Pedersen and Johnsen, 2017). Considering these quotas, it is possible to set a reference for the assessment of these nutrients as limiting factors, using tissue N and P contents and its ratio in opportunistic bloom forming seaweeds as an indicator of nutrient and relative nutrient enrichment (Cohen and Fong, 2006; Lourenço et al., 2006; Lyngby et al., 1999).

It is crucial to identify the primary sources of nutrients entering a water body in order to propose effective management strategies to reduce the negative effects of eutrophication (Kamer et al., 2004; Robertson and Savage, 2018; Thornber et al., 2008). The isotopic ratio between ^{14}N and the less abundant ^{15}N (i.e. $\delta^{15}\text{N}$) in marine macrophytes is often considered to assess the relative importance of nutrient sources with different isotopic signatures (e.g. García-Marín et al., 2013; Lin and Fong, 2008; Piñón-Gimate et al., 2017). These two stable isotopes can be differentially affected by physical, chemical or biological processes leading to distinctive isotopic signatures for different nitrogen sources. For instance, the use of lighter isotopes (^{14}N) can be favoured over the heavier ones (^{15}N) during certain metabolic processes (i.e. isotopic fractionation), which results in the gradual enrichment in heavy isotopes in the case of the reactants and the depletion of heavier isotopes in the case of the product (Mariotti et al., 1981; Viana and Bode, 2013). Sources of nitrogen such as urban wastewaters, manure or terrestrial runoff are usually more enriched in ^{15}N than seawater (Bateman and Kelly, 2007; Cohen and Fong, 2006; Costanzo et al., 2001) because of nitrification and volatilization of NH_4^+ , or denitrification of NO_3^- (Montoya, 2008). Overall the $\delta^{15}\text{N}$ value of macroalgae gives a more integrated and less transient response reflecting the importance and variability of nitrogen sources providing more information on nutrient enrichment than the $\delta^{15}\text{N}$ value of water samples (Viana and Bode, 2013, 2015). However, certain processes such as the differential affinity for different forms of nitrogen (e.g. NH_4^+ vs. NO_3^-), or isotopic fractionation needs to be considered when interpreting $\delta^{15}\text{N}$ values in macroalgae (Gröcke et al., 2017; Thornber et al., 2008; Viana et al., 2011).

Considering the key role of nutrient over-enrichment in the development of macroalgal blooms (Valiela et al., 1997; Smetacek and Zingone, 2013), identifying the limiting nutrient and the primary nutrient sources are necessary steps in order to define effective management strategies. In this context, this study aimed: i) to detect possible differences in the ecophysiological variables of interest for biomonitoring between tubular and laminar morphologies of *Ulva*; ii) to describe annual temporal dynamics of tissue nutrient contents and biomass; iii) to assess nutrient limitation; and iv) to identify the most likely sources of nitrogen in three large green tides occurring in Ireland.

2. Material and methods

2.1. Study area

Three nutrient enriched estuaries affected by large intertidal green tides (Bermejo et al., 2019b, 2020; Wan et al., 2017) were studied in Ireland: the Argideen, the Clonakilty and the Tolka (Fig. 1). All these estuaries were mesotidal (between 3.7 and 4.4 m), shallow (median depth between 3.7 and 2.1 m), and sheltered areas. The areas affected by macroalgal blooms in these estuaries were muddy and had a relatively high percentage of organic matter content (between 2.5 and 7.5%; Bermejo et al., 2019a). The estimated residence times were 4 days for the Argideen, 5.4 days for the Tolka and 7.5 days for Clonakilty. The shape of the Argideen and the area affected by macroalgal blooms in the Tolka estuary (i.e. the south lagoon of the North Bull Island) are elongated and progressively wider close to the mouth. Clonakilty is similar in shape to a bay or coastal lagoon, being wider in the middle and narrower

at the mouth (Fig. 1).

The catchments of the Argideen and the Clonakilty estuaries located on the southwest coast of Ireland are dominated by an agricultural landscape. In both cases, a wastewater treatment plant (WWTP) is present in the area. In the case of the Argideen and its associated rivers, nutrient loadings from the catchment were mainly from agricultural run off and these were estimated in 1,036,388 kg N y⁻¹ and 14,297 kg P y⁻¹ for 2016 (McGovern et al., 2020). Nitrogen and phosphorous loadings from the Courtmacsherry WWTP were estimated at 1460 kg y⁻¹ and 113 kg y⁻¹. In the case of Clonakilty, this system receives fresh water inputs from two streams, the Ashgrove and the Clonakilty, which in 2016 contributed an estimated total N loading of 135,034 kg y⁻¹, and total P loading of 623 kg y⁻¹ (McGovern et al., 2020). In the case of the WWTP at Clonakilty total N and total P loads in 2016 were estimated at 27,112 kg y⁻¹ and 1480 kg y⁻¹ respectively (Irish Waters, 2016).

The Tolka estuary on the East coast of Ireland is located in Dublin Bay, a complex system comprising of an open bay, estuaries and lagoons,

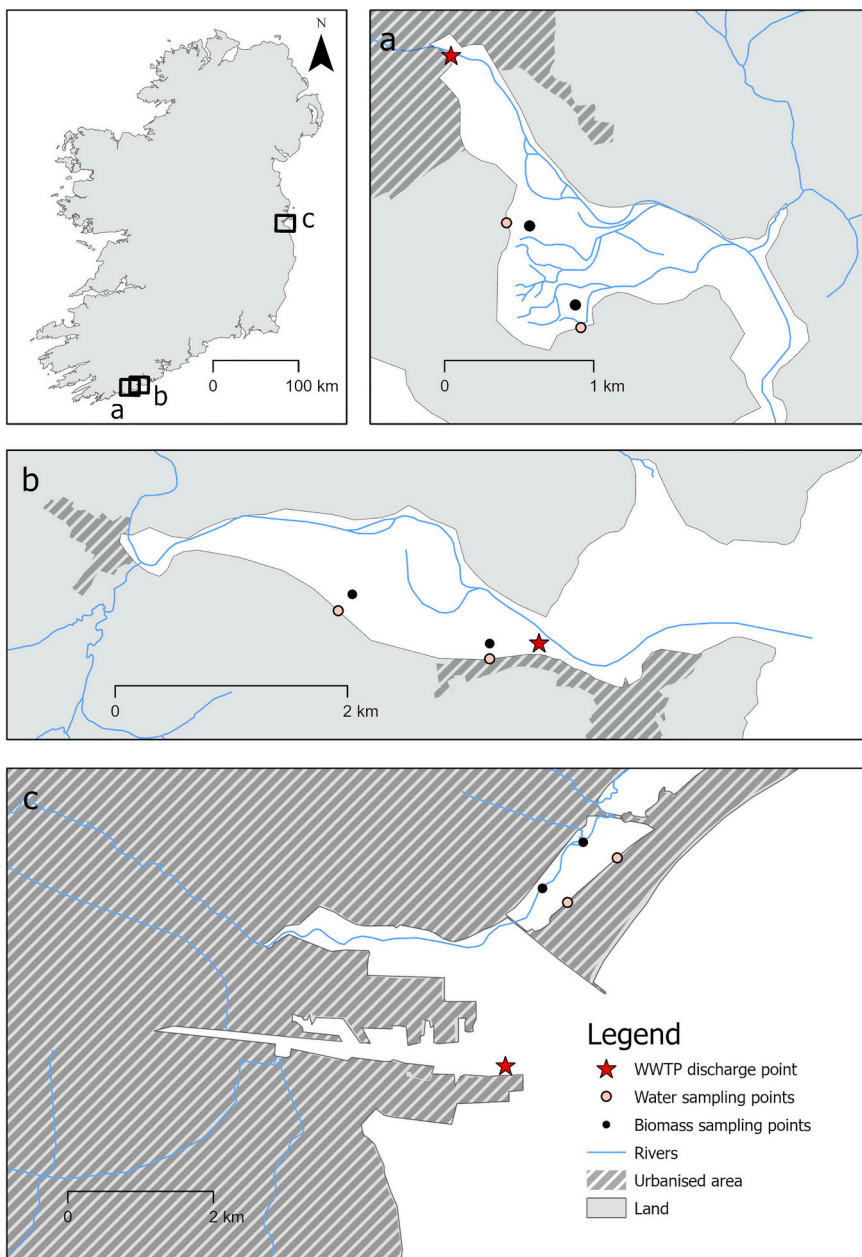


Fig. 1. Geographical location of the three estuaries studied in Ireland. Detailed map of (a) the Argideen, (b) the Clonakilty, and (c) the Tolka estuaries showing the position of the different sites within each estuary.

where the metropolitan area of Dublin dominates the landscape. The major nutrient inputs in this bay are the River Liffey (annual N load 825,947 Kg y⁻¹; annual P load 10,776 Kg y⁻¹) and the main WWTP located at Ringsend (annual N load 2,680,900 Kg y⁻¹; annual P load 437,256 Kg y⁻¹) (McGovern et al., 2020). The primary source of nitrogen in the River Liffey is from wastewater, followed by emissions from pasture. The Tolka (annual N load 87,994 Kg y⁻¹; annual P load 4353 Kg y⁻¹) and the Dodder (annual N load 118,720 Kg y⁻¹; annual P load 1460 Kg y⁻¹) rivers also have a significant contribution toward the total nutrient input in this bay. The nutrient enrichment of the River Tolka is mainly produced by diffuse agriculture sources, and by urban sources in the Dodder (McGovern et al., 2020). The study area, the south lagoon of North Bull Island which is part of the Tolka estuary, has been historically affected by large macroalgal blooms (Jeffrey et al., 1995). The sheltered nature of the area and the hydrodynamics of this bay, with predominant currents in a clockwise direction may have favoured the development of macroalgal blooms in the northern part of Dublin Bay, including the south lagoon of North Bull Island (Jeffrey et al., 1995).

2.2. Field sampling

Between June 2016 and August 2017, the Tolka and the Argideen were sampled on seven occasions, and the Clonakilty on six occasions. All the estuaries were sampled within a maximum period of one week to avoid temporal variation that may confound any spatial comparisons. For logistical reasons, the first sampling occasion was performed within a period of two months, and during this sampling occasion water samples were not collected.

On each sampling occasion and at each estuary, samples of water and seaweeds were collected at two sites within the estuary (Fig. 1), one close to the open sea ("outer") and another approximately one kilometre upstream ("inner"). For the assessment of biomass abundance, 12 replicates were collected per site on each sampling occasion at low tide in the inner part of the bloom during the maximum extension in the Argideen and the Tolka, and between 6 and 9 replicates at Clonakilty. In cold-temperate North Eastern Atlantic estuaries the period of largest spatial extent of the bloom occurs between June and August (e.g. Bermejo et al., 2020; Jeffrey et al., 1995; Scanlan et al., 2007). Using Google Earth images of maximum bloom extension from previous years, sampling stations were pre-determined. The sampling stations were located in the field using a Geographical Position System (GPS; Magellan Triton 400; 20 m error). Each replicate consisted of a quadrat of 25 × 25 cm. All living material present in each quadrat was collected, placed in a labelled plastic bag and transported to the laboratory.

To monitor water physicochemical characteristics (i.e. salinity and dissolved inorganic nutrients), water samples were collected during the previous or subsequent high tide following the biomass assessment. These samples were collected from the coast at a depth of 20 cm. Salinity was determined "in situ" using a hand refractometer (ATAGO S-20E, Tokyo, Japan). Six replicates samples of water per site (Fig. 1) were collected for the determination of different forms of dissolved inorganic nutrients. Each replicate sample consisted of 50 mL of filtered water. Samples were filtered "in situ" using a syringe and a nylon disposable filter (pore size 0.45 µm; Sarstedt, Germany). After filtration, samples were kept refrigerated in dark conditions and transported to the laboratory, where they were store at -20 °C prior to analysis.

2.3. Biomass sample processing

Once in the laboratory seaweed biomass was rinsed with freshwater to remove sediments, debris and other organisms. Because of the difficulties for accurate taxonomic identification of *Ulva* specimens based on morphological traits (Guidone et al., 2013; Malta et al., 1999) and the large quantities of biomasses processed, those specimens were sorted on laminar (mainly *Ulva rigida* C. Agardh; Bermejo et al., 2019a) and tubular (mainly *Ulva compressa* Linnaeus and *Ulva prolifera* O.F. Müller;

Bermejo et al., 2019a) morphologies. These biomasses were weighted after removing excess water using a salad spinner in order to obtain the fresh weight (FW) for each morphology. When possible, three independent subsamples of 5 g FW of *Ulva* per site, morphology and sampling occasion were freeze dried and stored in a desiccator until further elemental analysis (i.e., tissue N and P content). During February 2017, although no *Ulva* was found in the tidal flats of the Tolka estuary, some specimens of *Ulva* cf. *compressa* and *U. cf. rigida* were found attached to small boulders or entangled within the saltmarsh vegetation in the most internal part of the lagoon. Three replicates of each species were collected, washed and freeze dried for elemental analyses. No suitable *Ulva* biomass was found in the Argideen during February 2017.

2.3.1. Tissue nutrient contents and δ¹⁵N determination

Tissue N content and δ¹⁵N were determined on freeze dried and ground sample using an elemental analyser Vario ISOTOPE Cube (Elementar Analysensysteme GmbH, Hanau) connected to an isotope ratio mass spectrometer Isoprime 100 (Isoprime Ltd., Cheadle Hulm). The analytical precision was 0.15%. Analyses were carried out in duplicates. Tissue P content of samples was determined on the dried and ground seaweed tissue after oxidation with boiling H₂SO₄ followed by spectrophotometric analysis (Murphy and Riley, 1962; Strickland and Parsons, 1968). In some replicates (6 from the Clonakilty and 4 from the Argideen) it was not possible to estimate tissue P content as there was not enough biomass after measuring tissue N and δ¹⁵N. These treatments were: tubular *Ulva* from the inner section in June 2016 and from the outer section in August 2016 for the Argideen; laminar *Ulva* from the outer section in August 2016 and from the inner section in June 2017, and tubular *Ulva* from the outer section in June 2016 and August 2016 for the Argideen.

2.3.2. Dissolved nutrient determination in water samples

Seawater samples analysed for total oxidised N (TON) concentrations were determined on a Thermo Aquakem discrete analyser (Thermo Scientific, Vantaa, Finland), with a detection limit of 0.25 mg L⁻¹ for total oxidised N. Samples were also analysed for NO₂⁻-N, NH₄⁺-N, and dissolved reactive phosphorus (DRP) on the same instrument and Nitrate-N (NO₃⁻-N) was calculated by subtracting NO₂⁻-N from TON. Dissolved inorganic nitrogen (DIN) was calculated by summing NO₃⁻-N, NO₂⁻-N and NH₄⁺-N.

2.4. Statistical analyses

Statistical analyses were performed using the R free software environment (R Development Core Team, 2017). In all statistical analyses, significance was set at 5% risk error.

2.4.1. Temporal and spatial patterns of variability in major Irish green tides

In order to assess temporal and spatial differences between sampling occasions and sections within estuaries in tissue N and P contents, and δ¹⁵N ratio, a two-way Analysis of Variance (ANOVA) was performed per estuary. The factors considered were "Sampling occasion" (six or seven levels: June or July 2016, August 2016, October 2016, February 2017, April 2017, June 2017 and August 2017), and "Site" (2 levels: inner and outer). Because laminar morphologies were not present in several sampling occasions and estuaries, and to avoid possible confounding effects between different morphologies and sampling occasions, only samples from tubular morphologies were considered. All variables accomplished normality and homoscedasticity assumptions according to Shapiro-Wilks and Levene's tests. Post hoc Tukey's test was used to compare between levels of relevant factors or combinations of factors.

In the case of biomass abundances of total, tubular and laminar morphologies of *Ulva*, robust two-way ANOVA for trimmed means (20% of trimming level) were used instead of classical ANOVA, as significant deviations from normality and homoscedasticity were observed for these variables. Robust ANOVA do not make assumptions regarding the

functional form of the probability distribution (Mair and Wilcox, 2020; Staude and Sheather, 1990) and can be used when data are non-normal and shows unequal variance (i.e. heteroscedasticity). The functions “t2way” and “mcp2atm” of the WRS2 (Mair and Wilcox, 2020) package for R free software environment (R Development Core Team, 2017) were used for general and post hoc comparisons, respectively.

2.4.2. Assessing differences between *Ulva* morphologies

In order to assess differences between tubular and laminar *Ulva* morphologies in $\delta^{15}\text{N}$ values, tissue N and P contents, *t*-tests were performed when both morphologies were present at the same sampling occasion and site within the estuary. Data were checked for normality and homoscedasticity according to Shapiro-Wilks and Levene’s tests. When departures from normality were observed for at least one of the two groups, a Wilcoxon signed-rank test was used instead of a *t*-test.

2.4.3. Identifying nitrogen and phosphorus limitation

To evaluate the role of N and P as limiting factors, the tissue N and P contents for each morphology, site within estuary and sampling occasions were compared with the critical (Q_c) and subsistence (Q_s) quotes determined in previous ecophysiological studies. The Q_c considered for nitrogen was 2.45% following Villares and Carballeira (2004), and for phosphorus it was established at 0.215% according to Hernández et al. (2008). In the case of the Q_s , a value of 0.81% was considered for nitrogen following Villares and Carballeira (2004), and a value of 0.05% was considered for phosphorus according to Hernández et al. (2008). One sample *t*-tests were performed to identify when tissue nutrient contents were lower than the critical or subsistence quotes. When data did not accomplish the normality assumption according to Shapiro-Wilks test, a one-sample Wilcoxon signed rank test was used instead of a one-sample *t*-test.

2.4.4. Differences in nitrogen sources

A four-way ANOVA was performed in order to assess the effects of Estuary (three levels: Argideen, Clonakilty and Tolka), Morphology (two levels: tubular and laminar), Year (two levels: 2016 and 2017) and Section (two levels nested in Estuary) in the $\delta^{15}\text{N}$ ratio. In this case, only August 2016 and June 2017 were considered in this analysis because during these sampling occasions the concentrations of dissolved nitrogen forms were the lowest and the isotopic fractionation associated with seaweed nutrient uptake was limited or absent (e.g. Thornber et al., 2008). Furthermore, during these sampling occasions it was possible to collect the two different *Ulva* morphologies in all the estuaries and sites within the estuary, which allowed for the assessment of the effect of all these four factors and its interactions in the $\delta^{15}\text{N}$ ratio.

2.4.5. Correlation between biotic and environmental variables

In order to identify the factors that better explain bloom development, Spearman’s correlations among the biotic (i.e. total biomass, tubular biomass, laminar biomass, tissue N, tissue P and N:P ratio) and environmental variables (DIN, DRP, Salinity, rainfall, solar radiation, maximum and minimum air temperature), and a principal component analysis (PCA) were performed. Regarding the PCA, it was based on biotic variables, and environmental variables were fitted later using the “envifit” function of the “Vegan” package in R (Team, 2017). To perform these analyses, the trimmed mean (20% of trimming level) biomass and the mean values of other biological variables for each site within the estuary and sampling occasion were used. Only complete biological and environmental datasets were considered for these analyses ($n = 30$).

Daily meteorological information (i.e. rainfall, solar radiation, maximum air temperature and minimum air temperature) was obtained from the Irish meteorological service (Met Éireann; <http://www.met.ie/>). In the case of the Tolka estuary all the climatological information was obtained from the meteorological station at Dublin Airport, located less than 10 km from this estuary. In the case of the Argideen estuary and Clonakilty, rainfall data were obtained from the closest pluviometric

stations (i.e. Ballinspittle –11 km- and Rosscarberry –20 km-, respectively). The data for solar radiation, maximum and minimum air temperature were linearly interpolated considering the distance from the sampling site to the two closest meteorological stations for Clonakilty and the Argideen (i.e. Sherkin Island, and Roche’s Point). Each climatological parameter (i.e., accumulated rainfall, solar radiation and maximum and minimum air temperatures) was calculated considering data from the week previous to each sampling occasion.

3. Results

3.1. Dissolved inorganic nutrients

The concentration of DIN in seawater at the three monitored estuaries followed a common temporal trend with the highest concentrations during winter and the lowest during summer coinciding with the peak bloom (Fig. 2a). During February, mean DIN concentrations were higher than $60 \mu\text{mol L}^{-1}$ for the Tolka and the Argideen, and approximately $25 \mu\text{mol L}^{-1}$ for the Clonakilty. During June and August, mean DIN varied between 5 and $15 \mu\text{mol L}^{-1}$ in the three estuaries. Overall, the Argideen and the Tolka showed higher DIN values than the Clonakilty. Nitrate was usually the dominant form of DIN for the Argideen and the Clonakilty, and both ammonium and nitrate were the most abundant forms of DIN in the Tolka (Table S1). No common temporal pattern was identified for the concentration of DRP (Fig. 2b). In the Argideen and the Clonakilty the concentrations were similar and constantly varying between 0.2 and $0.7 \mu\text{mol L}^{-1}$. The DRP concentration in the Tolka was higher than in the other two estuaries, ranging from 0.9 to $2.0 \mu\text{mol L}^{-1}$ throughout the year. Water DIN:DRP ratio ranged from 2 to 75 in the Tolka, from 15.6 to 110.9 in the Clonakilty, and from 20.4 to 161.2 in the Argideen. This elemental ratio followed a temporal dynamic mimicking the DIN pattern (Fig. 2c). Finally, in the case of salinity no common temporal pattern arises (Fig. 2d). In general terms, the areas affected by green tides in the Argideen, Clonakilty and the Tolka showed similar values of salinity, ranging between 28 and 34‰ throughout the year. The lowest salinity values (approx. 23‰) were observed in the Tolka during February 2017.

3.2. Spatial and temporal dynamics of bloom biomass

The results of the robust two-way ANOVA for trimmed means of total, tubular and laminar biomass abundance revealed significant differences among sampling occasions for the three estuaries studied (Table 1). Differences between sites were only found in the Clonakilty in the case of the laminar morphology. Significant interactions between the factors “sampling occasion” and “site” were observed in the Clonakilty for total and laminar abundances, in the Tolka for total and tubular biomass, and in the Argideen for all biomass abundances assessed. However, as can be observed in Fig. 3 and as suggested by *Q*-values (Table 1), most of the variability was explained by sampling occasions rather than by the interaction between site and sampling occasion. In all the cases, the minimum total biomass abundances were recorded during February 2017 (Fig. 3a). Total biomass abundances close to 70 g FW m^{-2} were observed during February in Clonakilty, while no biomass was recorded in the Tolka and Argideen. In the case of the Tolka the highest total biomass abundances occurred between June and October ($4674 \pm 685 \text{ g FW m}^{-2}$ in June 2016; $1939 \pm 178 \text{ g FW m}^{-2}$ in August 2017). In the Argideen, the peak of total biomass abundance was observed between June and August ($2578 \pm 338 \text{ g FW m}^{-2}$ in June 2016; $1345 \pm 222 \text{ g FW m}^{-2}$ in August 2017), with significant lower values during October and April. The Clonakilty showed a different temporal pattern with the highest total biomass abundances recorded during April 2017 ($1641 \pm 391 \text{ g FW m}^{-2}$). Overall, tubular morphologies were more abundant than laminar morphologies. Mean biomass abundances were exceeded 1000 g m^{-2} during summer in three estuaries studied.

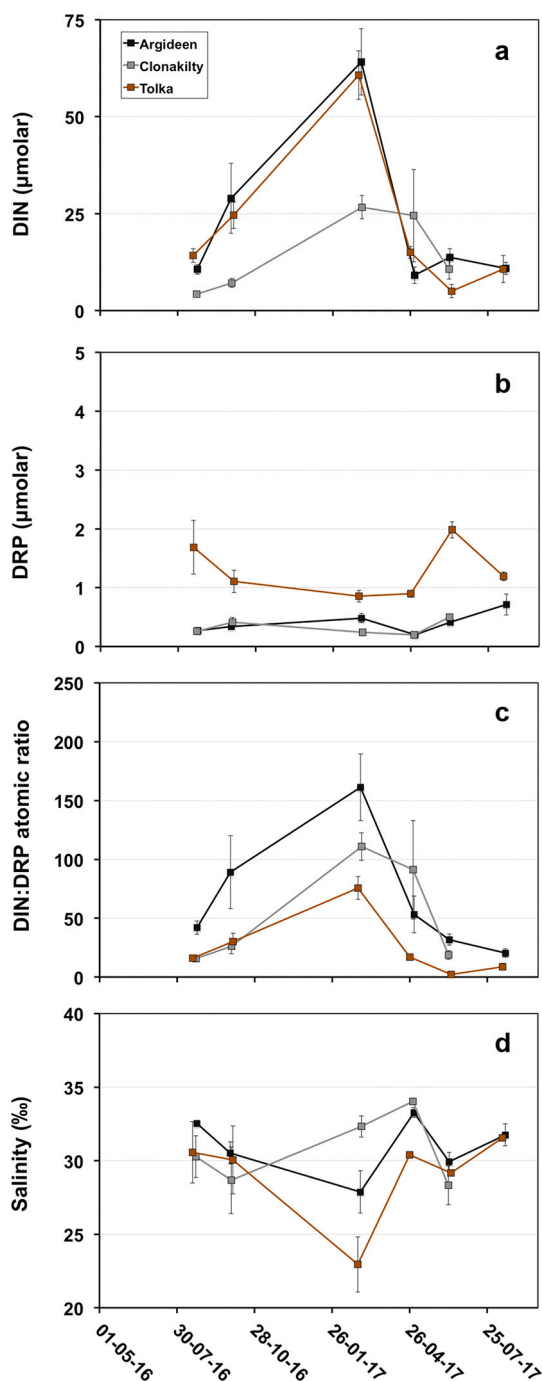


Fig. 2. Mean values of DIN (a), DRP (b), N:P atomic ratio (c) and salinity (d) according to Estuary and Sampling occasion. Mean \pm standard deviation, $n = 12$, except for salinity when $n = 4$.

3.3. Spatial and temporal dynamics of tissue N and P contents, and $\delta^{15}\text{N}$

The ANOVA (Table 2) revealed a significant temporal variability in the tubular *Ulva* tissue N content, but no differences between sites or interaction between site and sampling occasion were observed. Clonakilty and the Tolka followed a common temporal pattern (Fig. 4a) with higher concentrations during the late bloom (i.e. October 2016) and winter (i.e. February 2017), and lower tissue N contents during the peak bloom (between June and August). The temporal dynamic of the Argideen was similar to the one described for Clonakilty and the Tolka, however, the lack of data during winter due to the absence of *Ulva* in February 2017 precluded further comparisons. Overall, consistent

Table 1

Results of the robust two-way ANOVA (20% of trimming level) for trimming means testing the effects of the factors ‘‘Sampling occasion’’ (SO) and ‘‘Site’’ (Si) on the total, tubular and laminar biomass abundance of *Ulva*.

	Argideen	Clonakilty	Tolka
Total	Q	Q	Q
SO	188.06***	80.42***	583.09***
Si	3.16	2.66	2.53
SoxSi	18.45*	13.71	25.19**
Tubular	Q	Q	Q
SO	237.49***	56.23***	551.09***
Si	3.13	0.34	2.75
SoxSi	60.99***	11.23	27.56**
Laminar	Q	Q	Q
SO	115.93***	93.92***	92.11***
Si	1.32	12.96**	0.39
SoxSi	20.19*	44.10***	8.24

* p-value <0.05.

** p-value <0.01.

*** p-value <0.001.

pattern of differences between estuaries was observed with higher tissue N contents in the Tolka, followed by the Argideen, with the lowest values found in Clonakilty (Fig. 4a).

Regarding the tubular *Ulva* tissue P content, the ANOVA (Table 2) for the three estuaries indicated significant differences between sampling occasions, however, no common temporal dynamic was observed between the three estuaries (Fig. 4b). In the case of the Tolka a significant interaction between site and sampling occasion was observed. No differences between sites within the estuaries were observed.

The two-way ANOVA for the three studied estuaries indicated significant temporal differences in the $\delta^{15}\text{N}$ ratio of tubular morphologies of *Ulva* in the cases of the Tolka and the Argideen, but no temporal differences were observed in Clonakilty (Table 2). No differences between sites or in the interaction between site and sampling occasion were found in any of the estuaries. Although, both estuaries, the Tolka and the Argideen, showed significant differences between sampling occasions in the $\delta^{15}\text{N}$ ratio of tubular *Ulva*, the range of variation was higher in the case of the Tolka. The $\delta^{15}\text{N}$ ratio varied in this estuary between 7.35 ± 2.91 in February 2017 and 13.33 ± 0.40 in August 2017, while in the case of the Argideen the $\delta^{15}\text{N}$ ratio ranged from a minimum of 8.61 ± 0.33 in April 2017 to a maximum of 10.19 ± 0.51 in August 2017. The $\delta^{15}\text{N}$ values in tubular *Ulva* from Clonakilty were relatively constant throughout the sampling campaign, with a mean annual value of 8.56 ± 0.79 (Fig. 4c).

3.4. Differences in tissue N and P contents, and $\delta^{15}\text{N}$ ratios between morphologies

In general terms, no differences in tissue N and P contents, and $\delta^{15}\text{N}$ ratios were found between tubular and laminar morphologies of *Ulva* collected at the same site within an estuary for a specific sampling occasion. In the case of the tissue N content, significant differences were observed in two of thirty-one pairwise comparisons. These differences were found in the outer site of the Tolka estuary during June 2016 ($t = 22.33$; p-value <0.001), and in the inner site of the Clonakilty during June 2017 ($t = 5.13$; p-value <0.05). In both cases, the tissue N content was higher in tubular than in laminar morphologies. The mean coefficient of variation for tissue N content in tubular morphologies was 18.64% ($\pm 13.84\%$) and 15.06% ($\pm 11.24\%$) for laminar morphologies. No differences in the tissue P content between *Ulva* morphologies were observed for any of twenty-seven pairwise comparisons tested. The mean coefficient of variation for tissue P content in tubular morphologies was 15.36% ($\pm 9.87\%$) and 20.12% ($\pm 11.73\%$) for laminar morphologies. Regarding $\delta^{15}\text{N}$ ratio, significant differences between morphologies were observed in one of thirty-one pairwise comparisons, in the outer site of the Tolka estuary during June 2016 ($t = 4.22$; p-value

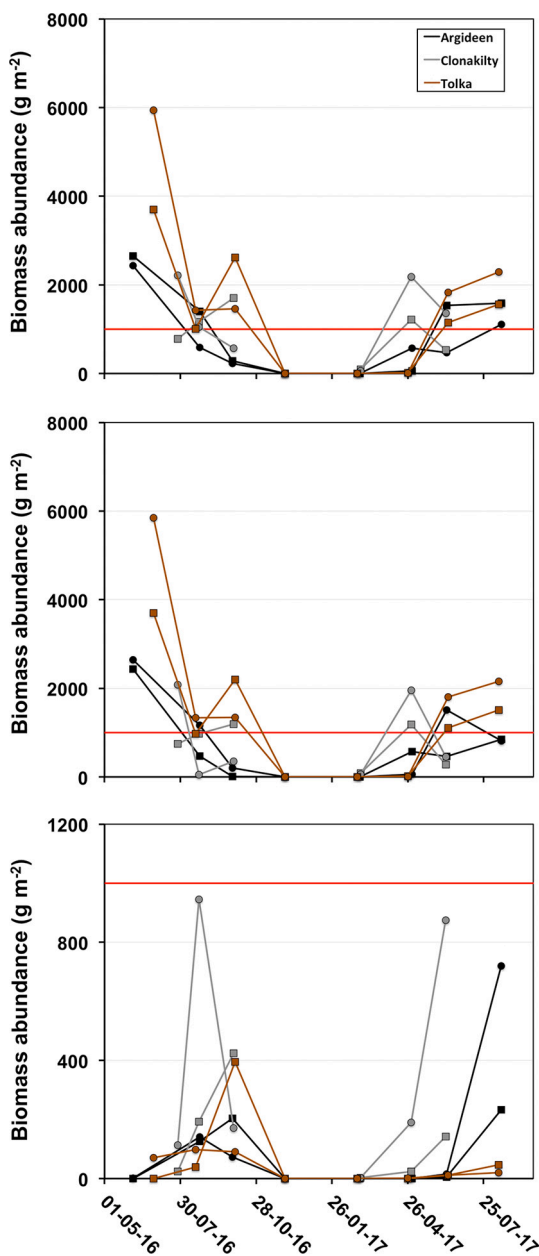


Fig. 3. Trimmed mean (20% trimming level) values of biomass (wet wt.) ($n = 12$ for the Argideen and Tolka, and $n =$ between 6 and 9 in the Clonakilty) of total (a), tubular (b) and laminar (c) morphologies of *Ulva* for each site (circles – outer sites; squares – inner sites) within estuary over six or seven different sampling occasions. The red line represent the biomass level of 1 kg m^{-2} established as the threshold between good and moderate status for the opportunistic macroalgal multimetric system to assess the ecological status of transitional water bodies in the context of the Water Framework Directive (Scanlan et al., 2007; Statutory Instrument (S.I.) 272/2009 -published in the “Iris Oifigiúil” of 24th July 2009-). (For interpretation of the references to colour in this figure legend, the reader is referred to the web version of this article.)

<0.001). The mean coefficient of variation for $\delta^{15}\text{N}$ ratio in tubular morphologies was 7.94% ($\pm 7.84\%$) and 8.09% ($\pm 8.77\%$) for laminar morphologies. Despite no significant differences between the tissue N and P content for most of the pairwise comparisons, tubular morphologies consistently yielded higher mean tissue N values (paired t -test = 3.46; $df = 30$; p -value <0.05 ; mean difference = 0.481%) and mean tissue P values (paired t -test = 2.51; $df = 26$; p -value <0.05 ; mean difference = 0.015%) when compared with laminar morphologies (Fig. 5). No biased differences between morphologies were found in the case of

the mean $\delta^{15}\text{N}$ ratio (paired t -test = -0.014 ; $df = 30$; p -value >0.05).

3.5. Nutrient limitation

Overall, the tissue N content of both *Ulva* morphologies was equal or higher than the critical quota (2.45% N; one sample t or Wilcoxon tests; p -value >0.05) on all sampling occasions, and sites within estuaries (Fig. 5a). The only exceptions were found in Clonakilty, where tubular *Ulva* showed a tissue N content lower than the critical quota during July 2016, and laminar *Ulva* yielded tissue N contents lower than the critical quota during July and August 2016.

In the case of the phosphorus (Fig. 5b), tissue values for this nutrient were always higher than the subsistence quota (0.05% P; one sample t -tests; p -value >0.05), but lower than the critical quota on most of the sampling occasions. In the Argideen estuary the tissue P content of tubular morphologies of *Ulva* was slightly higher or equal to the critical quota during August 2016 and during October 2016 for laminar morphologies. In Clonakilty both morphologies showed tissue P contents slightly higher or equal to the critical quota in February 2017, as well as during October 2016 in the case of the tubular *Ulva*, and in August 2016 in the case of the laminar form. Finally in the Tolka estuary, tissue P contents higher or equal to the critical quota were found in June 2016 for both morphologies as well as in October 2016 and April 2017 for tubular and laminar *Ulva*, respectively.

Overall, the atomic N:P ratio was higher than 30, suggesting nutritional disequilibrium (an equilibrate N:P ratio is higher than 10 and lower than 30; Fig. 4d), supporting the idea that *Ulva* had a nutritional status which tended toward P-limitation rather than N-limitation at all the estuaries in this study.

3.6. Nitrogen sources

The four-way ANOVA (Table 3) results revealed significant differences in the $\delta^{15}\text{N}$ ratio of *Ulva* between estuaries and in the interaction between estuary and year. No differences were observed between morphologies, sites within estuaries, or in other interactions between factors rather than the one between year and estuary previously mentioned. Overall, the Tolka yielded higher $\delta^{15}\text{N}$ ratios (12.50) than the Argideen (9.18) and Clonakilty (8.18), which showed similar ratios. The significant interaction is related with the temporal differences observed in the $\delta^{15}\text{N}$ ratio at Clonakilty, which yielded lower values during 2016 (7.70 ± 0.84) than in 2017 (8.67 ± 0.61). No differences between years were found at the Argideen and the Tolka (Fig. 6).

3.7. Correlations between biotic and environmental variables

The first two components of the PCA based on biotic variables explained over 66.77% of the total variation (Fig. 7). The score plot revealed that samples cluster by sampling occasion rather than by estuary, suggesting a common temporal pattern. Overall, data from August 2016, June 2017 and August 2017 were characterised by low tissue nitrogen contents and high biomasses. Within this group, samples from June 2017 (yellow markers in Fig. 7) showed higher N:P ratios than samples from August 2016 and 2017 (light and dark red markers in Fig. 7) due to low tissue P contents. Samples collected in Clonakilty during April 2017 (green markers in Fig. 7) showed high biomass abundances and low tissue nitrogen contents, similarly to samples collected during June 2016, August 2016 and 2017. Samples collected in April 2017 in the Tolka and the Argideen, and samples collected during October 2016 and February 2017 (grey and white markers in Fig. 7) showed high tissue N contents. Regarding this cluster, October 2016 showed higher biomass abundances than February and April 2017. The “envfit” function and Spearman correlations between biotic and environmental variables suggested an important effect of climatological conditions (i.e., solar radiation, rainfall, maximum and minimum air temperatures) on the ecophysiological status of green tides (i.e., tissue N

Table 2Results of the two-way ANOVA assessing the effects of the factors “Sampling occasion” (SO) and “Site” (Si) on the tissue N and P content, and $\delta^{15}\text{N}$ of *Ulva*.

Tissue N	Argideen			Clonakilty			Tolka		
	df	MS	F	df	MS	F	df	MS	F
SO	5	1.52	3.49*	5	8.43	20.16***	6	3.48	3.22*
Si	1	1.22	2.80	1	0.41	0.98	1	1.66	1.54
SoxSi	5	0.16	0.36	5	0.69	1.66	5	0.91	0.85
Res.	24	0.44		24	0.42		26	1.08	

Tissue P	df	MS ($\times 10^3$)	F	df	MS ($\times 10^3$)	F	df	MS ($\times 10^3$)	F
SO	5	3.11	3.02*	5	15.15	19.59***	6	6.44	7.51***
Si	1	1.65	1.61	1	1.16	1.50	1	0.19	0.22
SoxSi	3	0.35	0.34	3	0.59	0.76	5	2.37	2.76*
Res.	20	1.03		20	0.77		26	0.86	

$\delta^{15}\text{N}$	df	MS	F	df	MS	F	df	MS	F
SO	5	2.11	12.70***	5	1.06	1.74	6	34.91	20.81***
Si	1	0.09	0.57	1	0.20	0.32	1	2.77	1.65
SoxSi	5	0.27	1.62	5	0.39	0.64	5	1.22	0.73
Res.	24	0.17		24	0.61		26	1.68	

*p-Value < 0.05; **p-value < 0.01; *** p-value < 0.001.

and P contents, N:P ratio and biomass) (Table 4 and Fig. 7). The “envfit” found significant correlations with biotic variables for solar radiation ($r^2 = 0.473$; p -value < 0.001), maximum air temperature ($r^2 = 0.302$; p -value = 0.007) and rainfall ($r^2 = 0.220$; p -value = 0.034); and marginal for minimum air temperature ($r^2 = 0.199$; p -value = 0.054) and salinity ($r^2 = 0.196$; p -value = 0.053).

The Spearman correlations (Tables 4 and S2) indicated that biomasses were significantly and positively correlated with maximum temperatures ($0.60 > \text{Rho} > 0.42$; p -values < 0.05), and negatively correlated with DIN concentration ($-0.11 > \text{Rho} > -0.25$). Tissue N content was significantly and positively correlated with DIN concentration, and exhibited negative and significant correlations with solar radiation, minimum air temperature and salinity. In the case of tissue P content, only radiation showed a negative and significant correlation ($\text{Rho} = -0.71$; p -value < 0.001). The tissue N:P ratio was significantly and negatively correlated with minimum air temperature and solar radiation. Total biomass was significantly and negatively correlated with tissue N content ($\text{Rho} = -0.37$; p -value = 0.042), but did not show a significant correlation with tissue P content ($\text{Rho} = -0.27$; p -value = 0.148) or tissue N:P ratio ($\text{Rho} = 0.04$; p -value = 0.824).

4. Discussion

4.1. Biomass abundances and composition

The analysis of the abundance and composition of *Ulva* biomass in the three estuaries affected by large green tides revealed that tubular morphologies were more persistent and showed greater biomass abundances than laminar *Ulva* morphologies in the three green tides studied (Fig. 3). Similar patterns of biomass composition have been observed in other Irish estuaries affected by macroalgal blooms during the summer and autumn of 2020 (i.e. Dungarvan and Malahide; pers. obs.). This dominance of tubular morphologies contrasts with the findings of previous ecophysiological experiments using British and Irish specimens of *Ulva*, which predicted higher growth rates for *U. lacinulata* (incorrectly known as *U. rigida* Agardh, check Hughey et al., 2021 for further information) than for *U. compressa* for the environmental conditions found in the study areas (Bermejo et al., 2019a; Taylor et al., 2001). In this context, this dominance of tubular morphologies can be partially explained by the higher transport rates of biomass out of the estuary expected for laminar morphologies, as tubular morphologies of *Ulva* are usually found anchored to the substrate due to the burial of their basal parts (Bermejo et al., 2019b; Schories and Reise, 1993) and laminar

morphologies are mostly found free floating or tangled in the tubular canopy (Coffaro and Bocci, 1997; Salomonsen et al., 1997). This is also supported by the patterns observed in their maximum abundances and the contribution of laminar morphologies to the total biomass during the peak bloom of laminar morphologies with greater values at Clonakilty (501.73 ± 227.22 g FW m^{-2} ; 58.27%) than in the Tolka (214.53 ± 44.50 g FW m^{-2} ; 12.93%) and the Argideen (368.93 ± 80.30 g FW m^{-2} ; 28.99%). Considering the shape of the three estuaries, tidal ranges and residence times, biomass exportation rates of free living seaweeds due to tidal currents are expected to be more important in the tidal mudflats of Argideen and the Tolka than at Clonakilty which is more suitable for the development of laminar *Ulva*. These findings suggest that hydrodynamic conditions might play a critical role in determining the morphological composition of green tides in mudflats, with high hydrodynamic conditions limiting the accumulation of unattached *Ulva* (Coffaro and Bocci, 1997; Salomonsen et al., 1997).

Overall, the three studied estuaries showed a clear and common temporal pattern with maximum annual abundances occurring in late spring (i.e. Clonakilty) and summer (i.e. Argideen and Tolka), and minimum biomasses during winter, as expected for cold-temperate estuaries (e.g. Jeffrey et al., 1995; Malta and Verschuure, 1997; Schreyers et al., 2021). The results obtained revealed that macroalgal bloom development starts in late winter early spring (i.e. March–April), and bloom biomass quickly increases during late spring and early summer (i.e. May–June). Subsequently biomass abundance remains more or less stable or slowly decreases over the summer and early autumn. Finally, during late autumn (i.e. September–October), bloom biomass sharply decreases with no measurable biomass found from December to February in the Tolka and the Argideen. Solar radiation and temperature were key factors explaining bloom development and seasonality (Table 4; Fig. 7). In the case of the Clonakilty, the earlier development of macroalgal blooms may be attributed to the presence of overwintering strands of *Ulva* biomass, which would boost the initial development of the bloom acting as a source of spores and vegetative propagules (Lotze et al., 1999, 2000; Rinehart et al., 2014). Regarding morphological composition, blooms were dominated by tubular morphologies during spring and early summer, and co-dominated by tubular and laminar morphologies in summer and early autumn (Fig. 3) as observed in previous studies (Bermejo et al., 2019b; Jeffrey et al., 1995). This temporal succession supports the idea that Irish blooms are comprised of different species with different ecological requirements as initially reported by Jeffrey et al. (1995) and more recently confirmed by Bermejo et al. (2019b) using molecular identification tools. The presence of different

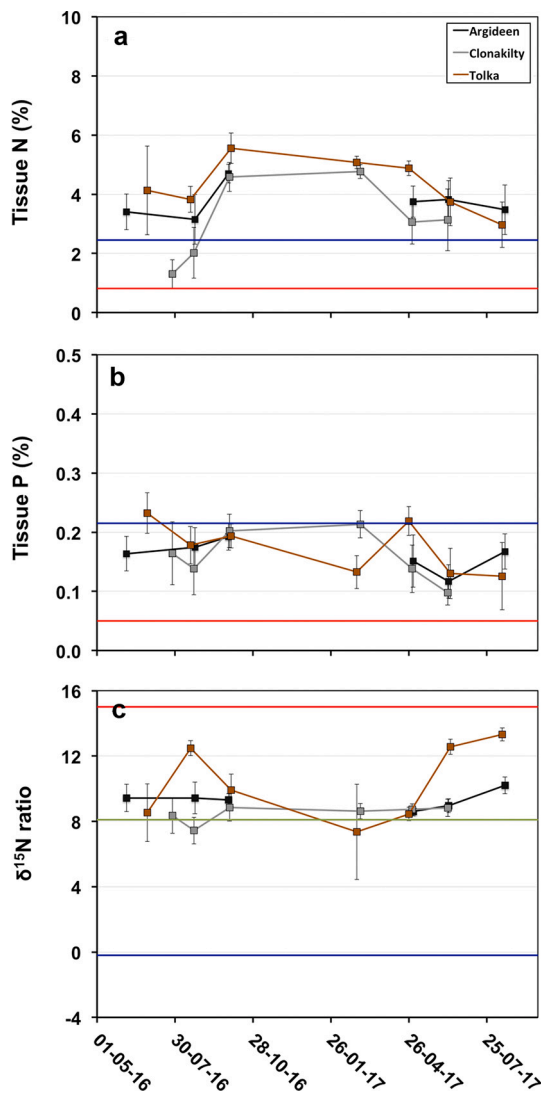


Fig. 4. Mean values of tissue N (a) and P (b) contents, and $\delta^{15}\text{N}$ (c) of tubular *Ulva* according to Estuary and Sampling occasion. Mean \pm standard deviation, $n = 6$. In Fig. 3a and b, the blue line represents the critical quota for N and P according to Villares and Carballeira (2004) and Hernández et al. (2008), and the red line the subsistence quota for N and P according to Hernández et al. (2008). In Fig. 3c, the red line indicated the mean nitrogen isotope values $\delta^{15}\text{N}$ for urban wastewaters (Cohen and Fong, 2006), the grey line the isotope values $\delta^{15}\text{N}$ for manure and compost (Bateman and Kelly, 2007), and the blue line the isotopic signature for synthetic fertilisers (Bateman and Kelly, 2007). (For interpretation of the references to colour in this figure legend, the reader is referred to the web version of this article.)

bloom forming species with different ecological requirements may promote seaweed tide persistence and extension under changing environmental conditions (Bermejo et al., 2020; Lavery et al., 1991; Yabe et al., 2009), which might be considered when designing management strategies or modelling bloom development, as possible shifts in bloom composition might have relevant implications for biomass balance in estuaries as well as for nutrient retention and exportation. In this sense, as pointed out by Bermejo et al. (2019a, 2019b) and Wan et al. (2017), *U. lacunculata* might be the main species contributing to laminar *Ulva* biomass in Irish green tides, and *U. compressa* and *U. prolifera* mostly accounting for tubular biomass.

4.2. Nutrient limitation

The temporal and spatial assessment of tissue N content in the three

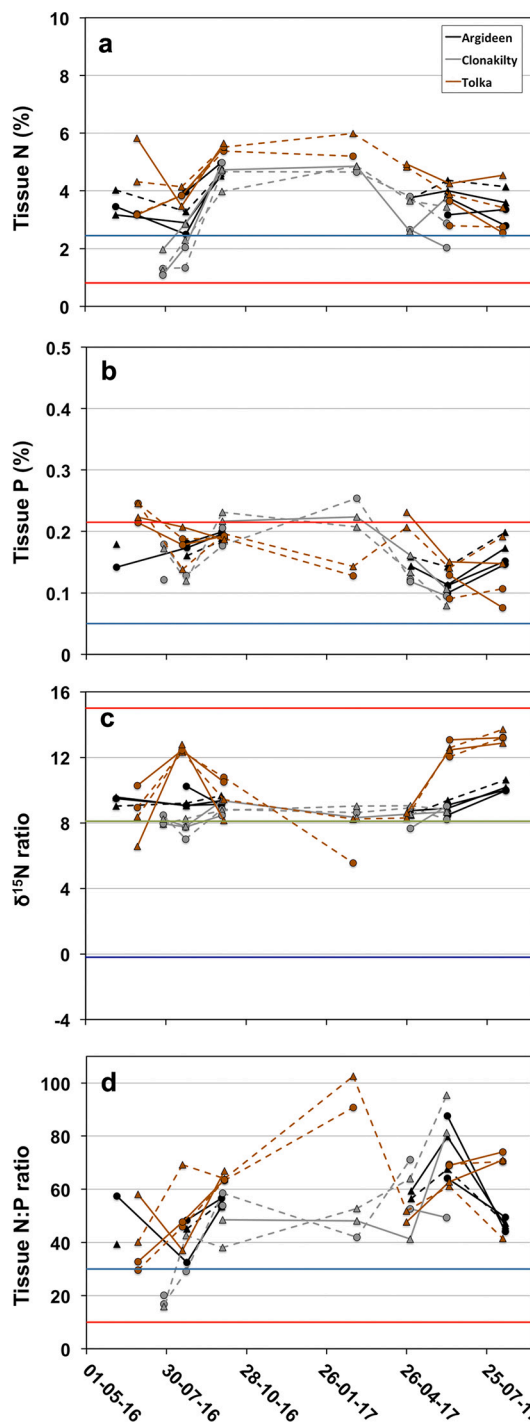


Fig. 5. Mean values of tissue N (a) and P (b) contents, and $\delta^{15}\text{N}$ (c) of tubular and laminar *Ulva* for each site within estuary and Sampling occasion. In Fig. 3a and b, the blue line represents the critical quota for N and P according to Villares and Carballeira (2004) and Hernández et al. (2008), and the red line the subsistence quota for N and P according to Hernández et al. (2008). In Fig. 3c, the red line indicated the mean nitrogen isotope values $\delta^{15}\text{N}$ for urban wastewaters (Cohen and Fong, 2006), the grey line the isotope values $\delta^{15}\text{N}$ for manure and compost (Bateman and Kelly, 2007), and the blue line the isotopic signature for synthetic fertilisers (Bateman and Kelly, 2007). (For interpretation of the references to colour in this figure legend, the reader is referred to the web version of this article.)

Table 3

Results of the four-way ANOVA assessing the effects of the factors “Year” (Y), “*Ulva* morphology” (Mor), Estuary (Est) and “Site” (Si(Est)) on the $\delta^{15}\text{N}$ of *Ulva*.

	df	MS	F
Y	1	0.72	1.85
Mor	1	0.27	0.69
Est	2	122.90	317.17***
Si(Est)	3	1.09	2.81
Y × Mor	1	0.01	0.03
Y × Est	2	3.06	7.89**
Mo × Est	2	0.34	0.88
Y × Si(Est)	3	0.05	0.12
Mor × Si(Est)	3	0.83	2.13
Y × Mor × Si(Est)	5	0.57	1.47
Res.	48	0.39	

*p-Value < 0.05; **p-value < 0.01; ***p-value < 0.001.

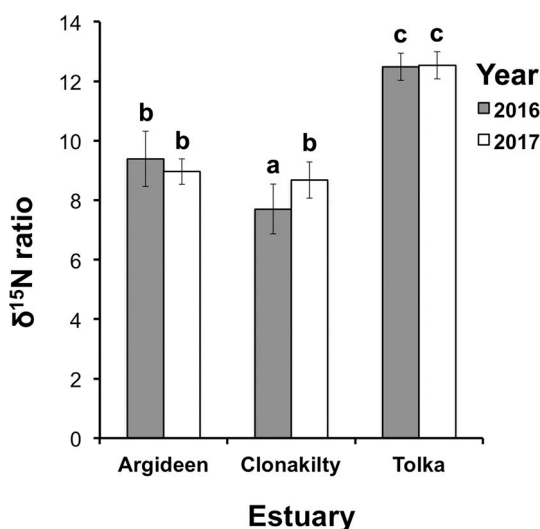


Fig. 6. Mean $\delta^{15}\text{N}$ of tubular and laminar *Ulva* in the three studied estuaries during August 2016 and June 2017. Mean \pm standard deviation, $n = 6$.

estuaries suggested no or little nitrogen limitation across any sampling occasion, sampling locations and morphological form of *Ulva* (Figs. 4 and 5), as generally tissue nitrogen content was higher than the critical quota determined by previous studies for *Ulva* spp. (Hernández et al., 2008; Pedersen and Borum, 1996; Villares and Carballeira, 2004). Only during the summer of 2016 tissue nitrogen tissue content was lower than the critical quota as observed at Clonakilty for tubular and laminar morphologies, indicating nitrogen limitation. The tissue N content showed a common temporal pattern in all the estuaries. A negative correlation between total biomass abundance and tissue N content was observed ($\text{Rho} = -0.37$; $p\text{-value} = 0.04$) suggesting a biomass dilution effect due to intensive growth during spring and early summer (e.g. Bermejo et al., 2019c; Hernández et al., 2006; Pedersen and Johnsen, 2017). The subsequent increase in tissue N content during the late bloom, when biomass abundance start to decrease, might be related with nutrient remineralisation as consequence of biomass decay and degradation, and a slower growth of *Ulva* (e.g. Bermejo et al., 2020). On the other hand, the results obtained suggested some phosphorus limitation as tissue phosphorus content was lower than the critical quota according to previous ecophysiological experiments (Hernández et al., 2008) (Figs. 4 and 5). This has important relevance for management strategies as, according to the theoretical relationship between seaweed growth and tissue nutrient content proposed by Hanisak (1983), the bloom development is expected to be more responsive to a change in phosphorus than in nitrogen availability. These tissue P contents observed are between the subsistence and critical quotas (i.e. deficient zone), and

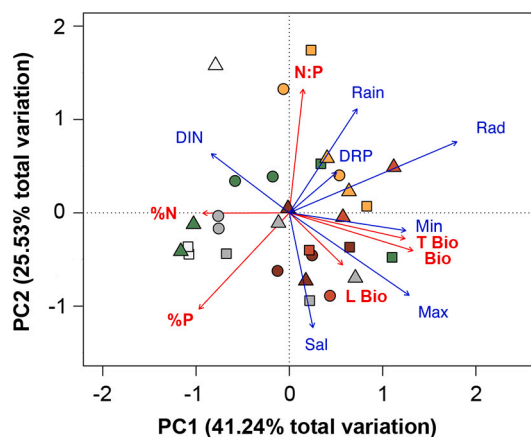


Fig. 7. Score biplot of the first and second principal component based on total biomass (Bio), tubular biomass (T Bio), laminar biomass (L Bio), tissue N (%N) and P (%P) contents, and tissue N:P (N:P) ratio (red arrows) of *Ulva* bloom for the different sites within the three studied estuaries (Argideen – dots; Clonakilty – squares; Tolka – triangles) and six of the seven sampling occasions (August 2016 - light red markers; October 2016 - grey markers; February 2017 - white markers; April 2017 - green markers; June 2017 - yellow markers; August 2017 - dark red markers). Blue arrows represent environmental variables fitted using “envfit” function of the Vegan package in R (accumulated rainfall - Rain; dissolved inorganic nitrogen - DIN; dissolved reactive phosphorous - DRP; maximum temperature - Max; minimum temperature - Min; salinity - Sal; solar radiation - Rad). (For interpretation of the references to colour in this figure legend, the reader is referred to the web version of this article.)

Table 4

Spearman correlations (Rho) between environmental and biotic variables. Rainfall - Accumulated rainfall; Max t - Maximum Air Temperature; Min t - Minimum Air Temperature; Rad - Solar radiation; DIN - Dissolved Inorganic Nitrogen; DRP - Dissolved Reactive Phosphorous; Sal - Salinity; N:P - tissue N:P ratio; %P - tissue P content; %N - tissue N content Bio - Total biomass; T Bio - Tubular biomass; L Bio - Laminar.

	Bio	T Bio	L Bio	N:P	%P	%N
Rainfall	0.07	-0.03	0.37*	0.05	-0.33	-0.26
Max t	0.60***	0.59***	0.42*	-0.02	-0.07	-0.18
Min t	0.24	0.10	0.62***	-0.21	-0.36	-0.62***
Rad	0.33	0.34	0.00	0.35	-0.71***	-0.63***
DIN	-0.25	-0.25	-0.11	0.05	0.26	0.44*
DRP	0.22	0.27	0.00	0.29	-0.05	0.18
Sal	0.06	0.11	-0.03	-0.50**	0.08	-0.42*

* p-value < 0.05.

** p-value < 0.01.

*** p-value < 0.001.

tissue N contents are higher than the critical quota (i.e. adequate zone). Thus, an enhanced growth of *Ulva* is expected to increased phosphorus availability, but a limited response is expected in the case of enhanced nitrogen availability (Fong et al., 1998; Hanisak, 1983). These observations partially validated the findings of McGovern et al. (2019), who identified phosphorus as the limiting factor constraining bloom development from April to September, and light as the factor constraining *Ulva* growth during the rest of the year based on a modelling approach.

4.3. Nutrient sources

Although no significant differences in tissue N and P content and in the $\delta^{15}\text{N}$ ratio were observed between *Ulva* morphologies collected within each site, across sampling occasion, mean tissue N and P contents were systematically higher in tubular than in laminar morphologies (paired $t\text{-test} > 2.51$; $p\text{-value} < 0.05$; Fig. 5). Two complementary hypotheses arise to explain these differences in the mean tissue nutrient

content between *Ulva* morphologies. The first hypothesis is that differences in tissue nutrient contents are likely a consequence of differences in growth rate, with species exhibiting lower growth rates having higher nutrient tissue contents, as this species would be less affected by dilution due to growth (Bermejo et al., 2019c; Hernández et al., 2006; Pedersen and Johnsen, 2017). This is supported by ecophysiological experiments performed by Taylor et al. (2001) and Bermejo et al. (2019a), which observed that *U. compressa* (one of the main species contributing to the biomass of tubular morphologies) yielded lower growth rates than *U. rigida* (the main species of laminar *Ulva* present in Irish estuaries) under the environmental conditions of these estuaries as mentioned earlier. The second hypothesis is that one of the morphologies may have access to a nutrient source that the other morphology does not have. The uptake of nutrients from porewaters by mud-entrained specimens of the red algae *Agarophyton chilensis* was demonstrated by Robertson and Savage (2018). Similarly, the burial of the basal part of tubular morphologies could provide access to nutrients from porewaters, which would not be equally available to laminar morphologies, which could partially explain the observed differences. Although the inexistence of differences in the $\delta^{15}\text{N}$ ratio between morphologies makes this second hypothesis less feasible, it cannot be ruled out, as the porewater and the seawater isotopic DIN signature could be similar.

Regarding the origin of nitrogen loadings, the $\delta^{15}\text{N}$ ratio observed in *Ulva* collected during the peak bloom, when DIN concentrations in water were at the lowest (Fig. 2) and isotopic fractionation is expected to be less relevant (Gröcke et al., 2017), followed the expected pattern with lower values in the Argideen and Clonakilty and higher values in the Tolka (Fig. 6). In the Argideen and the Clonakilty, where the catchment was dominated by agricultural land uses, the $\delta^{15}\text{N}$ ratio were close to the mean values observed for manure and compost (8.1‰; Bateman and Kelly, 2007). In the Tolka where the landscape was dominated by an urban centre, the isotopic signature of *Ulva* exceeded 10‰ and it was closer to the $\delta^{15}\text{N}$ values expected for seaweeds growing in environments N enriched by urban wastewaters or in highly urbanised catchments (15‰; Cohen and Fong, 2006; Piñón-Gimate et al., 2017).

The low $\delta^{15}\text{N}$ values observed in the tubular *Ulva* form late summer to early spring in the Tolka (Fig. 4c) could be explained by a more significant isotopic fractionation during these months (Gröcke et al., 2017; Thornber et al., 2008; Viana and Bode, 2015), when the DIN concentrations are high and *Ulva* biomass uptake is expected to be lower due to limited seaweed growth or low biomass abundance. This might have led to a higher selection of light isotopes during this period of high DIN concentrations and low nitrogen requirements (Dudley et al., 2010; Gröcke et al., 2017; Raimonet et al., 2013). A similar temporal pattern of variability in the isotopic signature of *Ulva*, with lower $\delta^{15}\text{N}$ ratio during winter and early spring followed by an increase in May, has been observed in other European mesotidal cold temperate estuary (Charente estuary, France; Raimonet et al., 2013). However, the low $\delta^{15}\text{N}$ values found during the peak bloom in June 2016 in the Tolka, when unusually high biomass abundances were measured, could be related with enhanced nutrient loadings coming from other sources different to urban wastewaters.

Regarding phosphorus, McGovern et al. (2020) identified stormwater run off from agriculture as the main source of phosphorus in the Argideen River and the Clonakilty Estuary, while wastewater was the main source in the Tolka accounting for 96% of phosphorus loading. Although stormwater run off from agriculture is the main source of phosphorus in the Argideen River and the Clonakilty Estuary, agricultural loadings are associated with increased rainfall. During drier periods in spring and summer, a critical period for green tide development in cold temperate estuaries (Bermejo et al., 2019b; Malta and Verschuure, 1997; Valiela et al., 1997), contributions by point source effluent discharges (e.g. domestic wastewaters, septic tanks) play a significant role maintaining baseflow concentrations of dissolved inorganic phosphorus (Jarvie et al., 2006; McGovern et al., 2019; Shore et al., 2017). Therefore, a reduction of these pressures could be crucial

for constraining bloom development especially during years with reduced rainfall in spring and summer. Furthermore, the reduction in these point sources will make it easier to assess the effectiveness of improvements in farm nutrient management practice (McGovern et al., 2019).

4.4. Implications for the biomonitoring of Irish green tides

The use of macroalgae as bioindicators to assess pollution in the marine environment has been proved successful in many ecological studies (Borowitzka, 1972; Orfanidis et al., 2003). Seaweeds have many desirable attributes as indicators of ecosystem integrity and environmental change, because they are: i) sensitive to different anthropogenic pressures, yielding an integrative response at different biological levels (from community structure to elemental composition; e.g. Bermejo et al., 2012, 2013; Lin and Fong, 2008); ii) ecologically and socially relevant (e.g. Bermejo et al., 2018; Cheminée et al., 2013; Mac Monagail and Morrison, 2020); iii) broadly extended along European coast (Lüning, 1990); and iv) present in almost all ecological situations (from pristine to highly degraded environment; Bermejo et al., 2012; Borowitzka, 1972; Juanes et al., 2008). For these reasons seaweeds are considered one of the biological quality elements proposed to assess the Ecological Status (ES) of coastal (e.g. Ballesteros et al., 2007; Bermejo et al., 2014; Wells et al., 2007) and transitional (e.g. Scanlan et al., 2007; Wilkinson et al., 2007) water bodies in the context of the Water Framework Directive (WFD, 2000/60/EC). Regarding transitional waters, the proposed indices to assess the ecological status such as the "opportunistic macroalgal multimetric system" (Scanlan et al., 2007) allow for the identification of problematic seaweed tides, but provide limited information about nutrient loads controlling bloom development.

During conditions of peak bloom, total biomass abundances of *Ulva* higher than 1 kg FW m⁻² were recorded in the three estuaries studied. This 1 kg FW m⁻² level of biomass is usually considered as the threshold at/or above where significant harmful effects on biota occur (Hull, 1987). For this reason, the "opportunistic macroalgal multimetric system" (Scanlan et al., 2007), which considers biomass abundance as one of the metrics to the assessment of the ES, establishes the threshold between the Good and Moderate Ecological Status in this abundance. This becomes particularly important considering legal implications when a good ES is not reached (European Commission 2000), as further management actions are necessary to reduce the total seaweed biomass and reach a good ES complying with obligations under the requirements of the WFD. In this context, the assessment of the nutrient status of problematic seaweed tides and the identification of nutrient sources become a tool supporting management strategies and regulations in order to control the development of macroalgal blooms caused by the anthropogenic nutrient over enrichment of aquatic ecosystems.

The findings of this study indicated that tubular and laminar morphologies of *Ulva* can be used indistinctly for the biomonitoring of nutrient limitation and sources in Irish seaweed tides as both morphologies yielded similar results about the nutrient status of the green tide for a determined sampling occasion and estuary (Figs. 5 and 6). If using one morphology, the tubular form provides more reliable spatial information as these are found anchored to the substrate, are easier to sample because they are more abundant and persistent, and provide a better insight of the nutrient status as they form the main component of the bloom in terms of biomass. However, previous studies showed that tubular morphologies comprise a large number and diversity of *Ulva* spp. in Irish estuaries, while in the case of laminar morphologies, most of the specimens belonged to *U. lacunculata* (Bermejo et al., 2019b; Fort et al., 2020; Wan et al., 2017) which might reduce variability associated with species specific differences in the uptake of nutrients or isotopes.

Regarding spatial and temporal dynamics of green tides in Ireland, the little differences found between sites within the estuary indicated that nutrient conditions might be similar along these estuaries of relative

small sizes (few kilometres) for a certain period, thus, no special attention needs to be taken when selecting an area for monitoring rather than avoiding to collect samples close to known sources of pollution (e.g. combined sewer overflow pipes) or the edge of the green tide. However, the important seasonal dynamics in tissue nutrient contents and $\delta^{15}\text{N}$ values make it necessary to consider temporal dynamics when designing sampling strategies (Table 2). Considering that bloom development in Ireland as in other cold-temperate estuaries might be limited by light and temperature during autumn and winter (Bermejo et al., 2019b; McGovern et al., 2019; Schreyers et al., 2021), and nutrient limitation might become more important just before the peak bloom or during the peak bloom, the period between May and July may be the most suitable time to assess nutrient limitation in Irish estuaries. Moreover, during these months isotopic fractionation in *Ulva* nitrogen uptake is expected to be less significant than previously stated, and differences in the isotopic signature of common nutrient sources in estuarine environments might be enhanced as a consequence of the increase in bacterial metabolism (Raimonet et al., 2013), which would more readily enable the identification of nitrogen sources (Gröcke et al., 2017; Thorner et al., 2008; Viana and Bode, 2015).

Finally, during peak bloom conditions, the *Ulva* arrangement in a canopy structure causes a gradient in environmental conditions (e.g. light, desiccation, nutrients). This gradient occurring at small scales and dependent on biomass abundance may result in marked vertical differences between the ecophysiological characteristics of the *Ulva* thallus located at the top or at the bottom of the canopy (Malta et al., 2003; Vergara et al., 1998). As the mixing of layers can produce biomass homogenization within the canopy (Malta et al., 2003), it is expected that a greater stratification of ecophysiological characteristics may exist with tubular morphologies of *Ulva* as these are usually anchored to the substrate and biomass mixing is less likely. These steep gradients can lead to differences in the limiting factors between the top and the bottom of the canopy. For instance, Malta et al. (2003) found that during the peak bloom the top layers of a *Ulva* canopy were limited by nutrients, while the bottom layers were limited by light, with both layer showing marked differences in ecophysiological characteristics. This canopy effect should be considered when sampling dense *Ulva* mats in order to avoid biases and non-representative assessment of the ecophysiological status of the bloom. In this case, a sample comprising the entire canopy with subsequent biomass homogenization is recommended for bioassessment.

CRedit authorship contribution statement

Ricardo Bermejo: Conceptualization, Methodology, Investigation, Formal analysis, Visualization, Writing – original draft, Funding acquisition, Project administration. **Nessa Golden:** Data curation, Visualization, Writing – original draft. **Elena Schrofner:** Data curation, Writing – original draft. **Kay Knöller:** Investigation, Methodology, Resources. **Owen Fenton:** Investigation, Methodology, Resources. **Ester Serrão:** Supervision, Writing – review & editing. **Liam Morrison:** Resources, Supervision, Writing – review & editing, Funding acquisition.

Declaration of competing interest

The authors declare that they have no known competing financial interests or personal relationships that could have appeared to influence the work reported in this paper.

Acknowledgements

This work has been co-financed under the 2014-2020 EPA Research Strategy (Environmental Protection Agency, Ireland), project no: 2015-W-MS-20 (the Sea-MAT Project) and project no: 2018-W-MS-32 (the MACRO-MAN Project), and the 2014-2020 ERDF Operational Programme and by the Department of Economy, Knowledge, Business and University of the Regional Government of Andalusia (Project reference:

FEDER-UCA18-106875). The authors are thankful to Moya O'Donnell, Maria Galindo-Ponce, Claudia Cara-Ortega, Micheal Mac Monagail, Ana Mendes, Charlene Linderhof, Nichole Keogh, Andrew Niven and Edna Curley for field assistance and Robert Wilkes for advice.

Appendix A. Supplementary data

Supplementary data to this article can be found online at <https://doi.org/10.1016/j.marpolbul.2021.113318>.

References

- Baden, S.P., Loo, L.O., Pihl, L., Rosenberg, R., 1990. Effects of eutrophication on benthic communities including fish: Swedish west coast. *Ambio* 19, 113–122. <https://doi.org/10.2307/4313676>.
- Ballesteros, E., Torras, X., Pinedo, S., García, M., Mangialajo, L., de Torres, M., 2007. A new methodology based on littoral community cartography dominated by macroalgae for the implementation of the European water framework directive. *Mar. Pollut. Bull.* 55, 172–180. <https://doi.org/10.1016/j.marpolbul.2006.08.038>.
- Bateman, A.S., Kelly, S.D., 2007. Fertilizer nitrogen isotope signatures. *Environ. Heal. Stud.* 43, 237–247. <https://doi.org/10.1080/10256010701550732>.
- Bermejo, R., Vergara, J.J., Hernández, I., 2012. Application and reassessment of the reduced species list index for macroalgae to assess the ecological status under the water framework directive in the Atlantic coast of southern Spain. *Ecol. Indic.* 12, 46–57. <https://doi.org/10.1016/j.ecolind.2011.04.008>.
- Bermejo, R., de la Fuente, G., Vergara, J.J., Hernández, I., 2013. Application of the CARLIT index along a biogeographical gradient in the Alboran Sea (European coast). *Mar. Pollut. Bull.* 72, 107–118. <https://doi.org/10.1016/j.marpolbul.2013.04.011>.
- Bermejo, R., Mangialajo, L., Vergara, J.J., Hernández, I., 2014. Comparison of two indices based on macrophyte assemblages to assess the ecological status of coastal waters in the transition between the Atlantic and Mediterranean eco-regions. *J. Appl. Phycol.* 26, 1899–1909. <https://doi.org/10.1007/s10811-013-0226-x>.
- Bermejo, R., Chefaoui, R.M., Engelen, A.H., Buonomo, R., Neiva, J., Ferreira-Costa, J., Pearson, G.A., Marbà, N., Duarte, C.M., Airoldi, L., Hernández, I., Guiry, M.D., Serrão, E.A., 2018. Marine forests of the Mediterranean-Atlantic *Cystoseira tamariscifolia* complex show a southern Iberian genetic hotspot and no reproductive isolation in Parapatry. *Sci. Rep.* <https://doi.org/10.1038/s41598-018-28811-1>.
- Bermejo, R., Heesch, S., Donnell, M.O., Golden, N., Mac Monagail, M., Edwards, M., Curley, E., Fenton, O., Daly, E., Morrison, L., 2019a. Nutrient dynamics and ecophysiology of opportunistic macroalgal blooms in Irish estuaries and coastal bays (sea-MAT). In: EPA Research Report no. 285. Wexford (Ireland): EPA.
- Bermejo, R., Heesch, S., Mac Monagail, M., O'Donnell, M., Daly, E., Wilkes, R.J., Morrison, L., 2019b. Spatial and temporal variability of biomass and composition of green tides in Ireland. *Harmful Algae* 81, 94–105. <https://doi.org/10.1016/j.hal.2018.11.015>.
- Bermejo, R., Macías, M., Cara, C.L., Sánchez-García, J., Hernández, I., 2019c. Culture of *Chondracanthus teedei* and *Gracilariaopsis longissima* in a traditional salina from southern Spain. *J. Appl. Phycol.* 31, 561–573. <https://doi.org/10.1007/s10811-018-1516-0>.
- Bermejo, R., MacMonagail, M., Heesch, S., Mendes, A., Edwards, M., Fenton, O., Knöller, K., Daly, E., Morrison, L., 2020. The arrival of a red invasive seaweed to a nutrient over-enriched estuary increases the spatial extent of macroalgal blooms. *Mar. Environ. Res.* 158, 104944.
- Björnsäter, B., Wheeler, P., 1990. Effect of nitrogen and phosphorous supply on growth and tissue composition of *Ulva fenestrata* and *Enteromorpha intestinalis* (Ulvaes, Chlorophyta). *J. Phycol.* 26, 603–611.
- Boesch, D.F., 2019. Barriers and bridges in abating coastal eutrophication. *Front. Mar. Sci.* 6, 123. <https://doi.org/10.3389/fmars.2019.00123>.
- Borowitzka, M.A., 1972. Intertidal algal species diversity and the effect of pollution. *Aust. J. Mar. Freshw. Res.* 23, 73–84.
- Cheminée, A., Sala, E., Pastor, J., Bodilis, P., Thiriet, P., Mangialajo, L., Cottalorda, J.-M., Francour, P., 2013. Nursery value of *Cystoseira* forests for Mediterranean rocky reef fishes. *J. Exp. Mar. Biol. Ecol.* 442, 70–79. <https://doi.org/10.1016/j.jembe.2013.02.003>.
- Coffaro, G., Bocci, M., 1997. Resources competition between *Ulva rigida* and *Zostera marina*: a quantitative approach applied to the lagoon of Venice. *Ecol. Model.* 102, 81–95.
- Cohen, R., Fong, P., 2006. Using opportunistic green macroalgae as indicators of nutrient supply and sources to estuaries. *Ecol. Appl.* 16, 1405–1420.
- Corzo, A., Van Bergeijk, S.A., García-Robledo, E., 2009. Effects of green macroalgal blooms on intertidal sediments: net metabolism and carbon and nitrogen contents. *Mar. Ecol. Prog. Ser.* 380, 81–93. <https://doi.org/10.3354/meps07923>.
- Costanzo, S.D., O'Donohue, M.J., Dennison, W.C., 2000. *Gracilaria edulis* (Rhodophyta) as a biological indicator of pulsed nutrients in oligotrophic waters. *J. Phycol.* 36, 680–685.
- Costanzo, S.D., O'Donohue, M.J., Dennison, W.C., Loneragan, N.R., Thomas, M., 2001. A new approach for detecting and mapping sewage impacts. *Mar. Pollut. Bull.* 42, 149–156.
- Critchley, A.T., Farnham, W.F., Morrell, S.L., 1986. An account of the attempted control of an introduced marine alga *Sargassum muticum*, in southern England. *Biol. Conserv.* 35, 313–332.

- Dudley, B., Barr, N., Shima, J., 2010. Influence of light intensity and nutrient source on $\delta^{13}\text{C}$ and $\delta^{15}\text{N}$ signatures in *Ulva pertusa*. *Aquat. Biol.* 9, 85–93. <https://doi.org/10.3354/ab00241>.
- Fletcher, R.L., 1996. The occurrence of “green tides” - a review. In: Schramm, W., Nienhuis, P.H. (Eds.), *Marine Benthic Vegetation: Recent Changes and the Effects of Eutrophication*. Springer, pp. 7–43.
- Fong, P., Boyer, K.E., Desmond, J.S., Zedler, J.B., 1996. Salinity stress, nitrogen competition and facilitation: what controls seasonal succession of 2 opportunistic green macroalgae? *J. Exp. Mar. Biol. Ecol.* 206, 203–221. [https://doi.org/10.1016/S0022-0981\(96\)02630-5](https://doi.org/10.1016/S0022-0981(96)02630-5).
- Fong, P., Boyer, K.E., Zedler, J.B., 1998. Developing an indicator of nutrient enrichment in coastal estuaries and lagoons using tissue nitrogen content of the opportunistic alga, *Enteromorpha intestinalis* (L. link). *J. Exp. Mar. Biol. Ecol.* 231, 63–79.
- Fort, A., Mannion, C., Fariñas-Franco, J.M., Sulpice, R., 2020. Green tides select for fast expanding *Ulva* strains. *Sci. Total Environ.* 698, 134337.
- Gao, S., Chen, X., Yi, Q., Wang, G., Pan, G., Lin, A., Peng, G., 2010. A strategy for the proliferation of *Ulva prolifera*, main causative species of green tides, with formation of sporangia by fragmentation. *PLoS One* 5, e8571. <https://doi.org/10.1371/journal.pone.0008571>.
- García-Marín, P., Cabaço, S., Hernández, I., Vergara, J.J., Silva, J., Santos, R., 2013. Multi-metric index based on the seagrass *Zostera noltii* (ZoNI) for ecological quality assessment of coastal and estuarine systems in SW Iberian Peninsula. *Mar. Pollut. Bull.* 68, 46–54. <https://doi.org/10.1016/j.marpolbul.2012.12.025>.
- Glibert, P.M., 2017. Eutrophication, harmful algae and biodiversity — challenging paradigms in a world of complex nutrient changes. *Mar. Pollut. Bull.* 124, 591–606. <https://doi.org/10.1016/j.marpolbul.2017.04.027>.
- Gröcke, D.R., Racionero-Gómez, B., Marschalek, J.W., Greenwell, H.C., 2017. Translocation of isotopically distinct macroalgae: a route to low-cost biomonitoring? *Chemosphere* 184, 1175–1185. <https://doi.org/10.1016/j.chemosphere.2017.06.082>.
- Guidone, M., Thornber, C., Wyssor, B., O’Kelly, C.J., 2013. Molecular and morphological diversity of Narragansett Bay (RI, USA) *Ulva* (Ulvales, Chlorophyta) populations. *J. Phycol.* 49, 979–995. <https://doi.org/10.1111/jpy.12108>.
- Hanisak, M.D., 1983. The nitrogen relationships of marine macroalgae. In: Carpenter, E. G., G. C.D. (Eds.), *Nitrogen in the Marine Environment*. Academic Press, New York, pp. 699–730.
- Hauxwell, J., Cebrian, J., Furlong, C., Valiela, I., 2001. Macroalgal canopies contribute to eelgrass (*Zostera marina*) decline in temperate estuarine ecosystems. *Ecology* 82, 1007–1022.
- Hayden, H.S., Blomster, J., Maggs, C.A., Silva, P.C., Stanhope, M.J., Waaland, J.R., Ydeni, H.S.H.A., Blomster, J., Maggs, C.A., Silva, P.C., Stanhope, M.J., Waaland, J. R., 2003. Linnaeus was right all along: *Ulva* and *Enteromorpha* are not distinct genera. *Eur. J. Phycol.* 38, 277–294. <https://doi.org/10.1080/1364253031000136321>.
- Hernandez, I., Peralta, G., Perez-Llorens, J.L., Vergara, J.J., Niell, F.X., 1997. Biomass and growth dynamics of *Ulva* species in Palmones River estuary. *J. Phycol.* 33, 764–772. <https://doi.org/10.1111/j.0022-3646.1997.00764.x>.
- Hernández, I., Pérez-Pastor, A., Vergara, J.J., Martínez-Aragón, J.F., Fernández-Engo, M.A., Pérez-Lloréns, J.L., 2006. Studies on the biofiltration capacity of *Gracilaria longissima*: from microscale to macroscale. *Aquaculture* 252, 43–53. <https://doi.org/10.1016/j.aquaculture.2005.11.048>.
- Hernández, I., Pérez-Pastor, A., Mateo, J.J., Megina, C., Vergara, J.J., 2008. Growth dynamics of *Ulva rotundata* (Chlorophyta) in a fish farm: implications for biomitigation at a large scale. *J. Phycol.* 44, 1080–1089. <https://doi.org/10.1111/j.1529-8817.2008.00550.x>.
- Howarth, R., Anderson, D., Cloern, J., Elfring, C., Hopkinson, C., Lapointe, B., Malone, T., Marcus, N., McGlathery, K., Sharpley, A., Walker, D., 2000. Nutrient pollution of coastal rivers, bays, and seas. *Issues Ecol.* 7, 1–15.
- Hughey, J.R., Gabrielson, P.W., Maggs, C.A., Mineur, F., 2021. Genomic analysis of the lectotype specimens of European *Ulva rigida* and *Ulva lacunculata* (Ulvaaceae, Chlorophyta) reveals the ongoing misapplication of names. *Eur. J. Phycol.* 00, 1–11. <https://doi.org/10.1080/09670262.2021.1914862>.
- Hull, S.C., 1987. Macroalgal mats and species abundance: a field experiment. *Estuar. Coast. Shelf Sci.* 25, 519–532. [https://doi.org/10.1016/0272-7714\(87\)90112-0](https://doi.org/10.1016/0272-7714(87)90112-0).
- Irish Waters, 2016. Annual environmental report. In: Agglomeration Name: Clonakilty and Environs; License Register No. D0051–01.
- Jarvie, H.P., Neal, C., Withers, P.J.A., 2006. Sewage-effluent phosphorus: a greater risk to river eutrophication than agricultural phosphorus? *Sci. Total Environ.* 360, 246–253. <https://doi.org/10.1016/j.scitotenv.2005.08.038>.
- Jeffrey, D.W., Brennan, M.T., Jennings, E., Madden, B., Wilson, J.G., 1995. Nutrient sources for in-shore nuisance macroalgae: the Dublin bay case. *Ophelia* 42, 147–161. <https://doi.org/10.1080/00785326.1995.10431501>.
- Juanes, J.A., Guinda, X., Puente, A., Revilla, J.A., 2008. Macroalgae, a suitable indicator of the ecological status of coastal rocky communities in the NE Atlantic. *Ecol. Indic.* 8, 351–359. <https://doi.org/10.1016/j.ecolind.2007.04.005>.
- Kamer, K., Fong, P., Kennison, R.L., Schiff, K., 2004. The relative importance of sediment and water column supplies of nutrients to the growth and tissue nutrient content of the green macroalga *Enteromorpha intestinalis* along an estuarine resource gradient. *Aquat. Ecol.* 38, 45–56. <https://doi.org/10.1023/B>.
- Krause-Jensen, D., Sagert, S., Schubert, H., Boström, C., 2008. Empirical relationships linking distribution and abundance of marine vegetation to eutrophication. *Ecol. Indic.* 8, 515–529. <https://doi.org/10.1016/j.ecolind.2007.06.004>.
- Lapointe, B.E., 1987. Phosphorus- and nitrogen-limited photosynthesis and growth of *Gracilaria tikvahiae* (Rhodophyceae) in the Florida keys: an experimental field study. *Mar. Biol.* 93, 561–568.
- Lavery, P.S., Lukatelich, R.J., McComb, A.J., 1991. Changes in the biomass and species composition of macroalgae in a eutrophic estuary. *Estuar. Coast. Shelf Sci.* 33, 1–22. [https://doi.org/10.1016/0272-7714\(91\)90067-L](https://doi.org/10.1016/0272-7714(91)90067-L).
- Lenzi, M., Gennaro, P., Renzi, M., Persia, E., Porrello, S., 2012. Spread of *Alsidium corallinum* C. ag. in a Tyrrhenian eutrophic lagoon dominated by opportunistic macroalgae. *Mar. Pollut. Bull.* 64, 2699–2707. <https://doi.org/10.1016/j.marpolbul.2012.10.004>.
- Lin, D.T., Fong, P., 2008. Macroalgal bioindicators (growth, tissue N, $\delta^{15}\text{N}$) detect nutrient enrichment from shrimp farm effluent entering Opunohu Bay, Moorea, French Polynesia. *Mar. Pollut. Bull.* 56, 245–249. <https://doi.org/10.1016/j.marpolbul.2007.09.031>.
- Littler, M.M., Littler, D.S., Phillip, R.T., 1983. Evolutionary strategies in a tropical barrier reef system: functional-form groups of marine macroalgae. *J. Phycol.* 19, 229–237.
- Lotze, H.K., Schramm, W., Schories, D., Worm, B., 1999. Control of macroalgal blooms at early developmental stages: *Pilayella littoralis* versus *Enteromorpha* spp. *Oecologia* 119, 46–54. <https://doi.org/10.1007/s004420050759>.
- Lotze, H.K., Worm, B., Sommer, U., 2000. Propagule banks, herbivory and nutrient supply control population development and dominance patterns in macroalgal blooms. *Oikos* 89, 46–58. <https://doi.org/10.1034/j.1600-0706.2000.890106.x>.
- Lotze, H.K., Worm, B., Sommer, U., 2001. Strong bottom-up and top-down control of early life stages of macroalgae. *Limnol. Oceanogr.* 46, 749–757. <https://doi.org/10.4319/lo.2001.46.4.0749>.
- Lourenço, S.O., Barbarino, E., Nascimento, A., Freitas, J.N.P., Diniz, G.S., 2006. Tissue nitrogen and phosphorus in seaweeds in a tropical eutrophic environment: what a long-term study tells us. *J. Appl. Phycol.* 18, 389–398. <https://doi.org/10.1007/978-1-4020-5670-3>.
- Lu, C., Tian, H., 2017. Global nitrogen and phosphorus fertilizer use for agriculture production in the past half century: shifted hot spots and nutrient imbalance. *Earth Syst. Sci. Data* 9, 181–192. <https://doi.org/10.5194/essd-9-181-2017>.
- Lüning, K., 1990. *Seaweeds: Their Environment, Biogeography, and Ecophysiology*. John Wiley & Sons, Inc.
- Lynghy, J.E., Mortensen, S., Ahrensberg, N., 1999. Bioassessment techniques for monitoring of eutrophication and nutrient limitation in coastal ecosystems. *Mar. Pollut. Bull.* 39, 212–223. [https://doi.org/10.1016/S0025-326X\(99\)00025-9](https://doi.org/10.1016/S0025-326X(99)00025-9).
- Mair, P., Wilcox, R., 2020. Robust statistical methods in R using the WRS2 package. *Behav. Res. Methods* 52, 464–488. <https://doi.org/10.3758/s13428-019-01246-w>.
- Malta, E.-J., Verschuure, J.M., 1997. Effects of environmental variables on between-year variation of *Ulva* growth and biomass in a eutrophic brackish lake. *J. Sea Res.* 38, 71–84. [https://doi.org/10.1016/S1385-1101\(97\)00039-7](https://doi.org/10.1016/S1385-1101(97)00039-7).
- Malta, E.-J., Draisma, S.G.A., Kamerlings, P., 1999. Free-floating *Ulva* in the Southwest Netherlands: species or morphotypes? A morphological, molecular and ecological comparison. *Eur. J. Phycol.* 34, 443–454. <https://doi.org/10.1017/S0967026299002474>.
- Malta, E., Rijstenbil, J.W., Brouwer, P.E.M., Kromkamp, J.C., 2003. Vertical heterogeneity in physiological characteristics of *Ulva* spp. *mar. Biol.* 143, 1029–1038. <https://doi.org/10.1007/s00227-003-1134-4>.
- Mariotti, A., Germon, J.C., Hubert, P., Kaiser, P., Letolle, R., Tardieux, A., Tardieux, P., 1981. Experimental determination of nitrogen kinetic isotope fractionation: some principles; illustration for the denitrification and nitrification processes. *Plant Soil* 62, 413–430. <https://doi.org/10.1007/BF02374138>.
- McGovern, J.V., Nash, S., Hartnett, M., 2019. Interannual improvement in sea lettuce blooms in an agricultural catchment. *Front. Mar. Sci.* 6, 64. <https://doi.org/10.3389/fmars.2019.00064>.
- McGovern, J.V., Nash, S., Hartnett, M., 2020. Modelling Irish Transitional and Coastal Systems to Determine Nutrient Reduction Measures to Achieve Good Status. EPA Research Report No. 359. EPA, Wexford (Ireland).
- Monagail, M. Mac, Morrison, L., 2020. The seaweed resources of Ireland: a twenty-first century perspective. *J. Appl. Phycol.* 32, 1287–1300. <https://doi.org/10.1007/s10811-020-02067-7>.
- Montoya, J., 2008. Nitrogen stable isotopes in marine environments. In: Capone, D.G., Bronk, D.A., Mulholland, M.R., Carpenter, E.J. (Eds.), *Nitrogen in the Marine Environment*. Academic Press, San Diego, pp. 1277–1302.
- Murphy, J., Riley, J.P., 1962. Determination of phosphate in natural waters. *Anal. Chim. Acta* 27, 31–36.
- Ní Longphuirt, S., O’Boyle, S., Wilkes, R., Dabrowski, T., Stengel, D.B., 2015. Influence of hydrological regime in determining the response of macroalgal blooms to nutrient loading in two Irish estuaries. *Estuar. Coasts* 39, 478–494. <https://doi.org/10.1007/s12237-015-0009-5>.
- O’Boyle, S., Trodd, W., Bradley, C., Tierney, D., Wilkes, R., Longphuirt, S.N., Smith, J., Stephens, A., Barry, J., Maher, P., McGinn, R., Mockler, E., Deakin, J., Craig, M., Gurrie, M., 2019. Water Quality in Ireland 2013–2018. EPA Report. EPA, Wexford (Ireland).
- Orfanidis, S., Panayotidis, P., Stamatis, N., 2003. An insight to the ecological evaluation index (EEI). *Ecol. Indic.* 3, 27–33. [https://doi.org/10.1016/S1470-160X\(03\)00008-6](https://doi.org/10.1016/S1470-160X(03)00008-6).
- Pedersen, M.F., Borum, J., 1996. Nutrient control of algal growth in estuarine waters. Nutrient limitation and the importance of nitrogen requirements and nitrogen storage among phytoplankton and species of macroalgae. *Mar. Ecol. Prog. Ser.* 142, 261–272.
- Pedersen, M.F., Johnsen, K.L., 2017. Nutrient (N and P) dynamics of the invasive macroalga *Gracilaria vermiculophylla*: nutrient uptake kinetics and nutrient release through decomposition. *Mar. Biol.* 164, 1–12. <https://doi.org/10.1007/s00227-017-3197-7>.
- Piñón-Gimate, A., Espinosa-Andrade, N., Sánchez, A., Casas-Valdez, M., 2017. Nitrogen isotopic characterisation of macroalgal blooms from different sites within a

- subtropical bay in the Gulf of California. *Mar. Pollut. Bull.* 116, 130–136. <https://doi.org/10.1016/j.marpolbul.2016.12.075>.
- Raimonet, M., Guillou, G., Mornet, F., Richard, P., 2013. Macroalgae $\delta^{15}\text{N}$ values in well-mixed estuaries: Indicator of anthropogenic nitrogen input or macroalgal metabolism? *Estuar. Coast. Shelf Sci.* 119, 126–138. <https://doi.org/10.1016/j.ecss.2013.01.011>.
- Rinehart, S., Guidone, M., Ziegler, A., Schollmeier, T., Thornber, C., 2014. Overwintering strategies of bloom-forming *Ulva* species in Narragansett Bay, Rhode Island, USA. *Bot. Mar.* 57, 337–341. <https://doi.org/10.1515/bot-2013-0122>.
- Robertson, B.P., Savage, C., 2018. Mud-entrained macroalgae utilise porewater and overlying water column nutrients to grow in a eutrophic intertidal estuary. *Biogeochemistry* 139, 1–16. <https://doi.org/10.1007/s10533-018-0454-x>.
- Salomonsen, J., Flindt, M.R., Geertz-Hansen, O., 1997. Significance of advective transport of *Ulva lactuca* for a biomass budget on a shallow water location. *Ecol. Model.* 102, 129–132.
- Scanlan, C.M., Foden, J., Wells, E., Best, M.A., 2007. The monitoring of opportunistic macroalgal blooms for the water framework directive. *Mar. Pollut. Bull.* 55, 162–171. <https://doi.org/10.1016/j.marpolbul.2006.09.017>.
- Schories, D., Reise, K., 1993. Germination and anchorage of *Enteromorpha* spp. in sediments of the Wadden Sea. *Helgoländer Meeresuntersuchungen* 47, 275–285.
- Schreyers, L., van Emmerik, T., Biermann, L., Le Lay, Y.-F., 2021. Spotting green tides over Brittany from space: three decades of monitoring with Landsat imagery. *Remote Sens.* 13, 1408. <https://doi.org/10.3390/rs13081408>.
- Sfriso, A., Marcomini, A., Pavoni, B., 1987. Relationships between macroalgal biomass and nutrient concentrations in a hypertrophic area of the Venice lagoon. *Mar. Environ. Res.* 22, 297–312. [https://doi.org/10.1016/0141-1136\(87\)90005-5](https://doi.org/10.1016/0141-1136(87)90005-5).
- Shore, M., Murphy, S., Mellander, P.E., Shortle, G., Melland, A.R., Crockford, L., O'Flaherty, V., Williams, L., Morgan, G., Jordan, P., 2017. Influence of stormflow and baseflow phosphorus pressures on stream ecology in agricultural catchments. *Sci. Total Environ.* 590–591, 469–483. <https://doi.org/10.1016/j.scitotenv.2017.02.100>.
- Smetacek, V., Zingone, A., 2013. Green and golden seaweed tides on the rise. *Nature* 504, 84–88. <https://doi.org/10.1038/nature12860>.
- Staudte, R.G., Sheather, S.J., 1990. *Robust Estimation and Testing*. John Wiley & Sons, Inc.
- Strickland, J., Parsons, T., 1968. *A Practical Handbook of Seawater Analysis*. Fisheries Research Board of Canada, Ottawa, Canada.
- Taylor, R., Fletcher, R., Raven, J., 2001. Preliminary studies on the growth of selected “green tide” algae in laboratory culture: effects of irradiance, temperature, salinity and nutrients on growth rate. *Bot. Mar.* 44, 327–336. <https://doi.org/10.1515/BOT.2001.042>.
- Team, R.C., 2017. *R: A Language and Environment for Statistical Computing*. R Foundation for Statistical Computing, Vienna, Austria. <https://www.R-project.org/>.
- Teichberg, M., Fox, S.E., Olsen, Y.S., Valiela, I., Martinetto, P., Iribarne, O., Muto, E.Y., Petti, M.A.V., Corbisier, T.N., Soto-Jiménez, M., Páez-Osuna, F., Castro, P., Freitas, H., Zitelli, A., Cardinaletti, M., Tagliapietra, D., 2010. Eutrophication and macroalgal blooms in temperate and tropical coastal waters: nutrient enrichment experiments with *Ulva* spp. *Glob. Chang. Biol.* 16, 2624–2637. <https://doi.org/10.1111/j.1365-2486.2009.02108.x>.
- Thornber, C.S., DiMilla, P., Nixon, S.W., McKinney, R.A., 2008. Natural and anthropogenic nitrogen uptake by bloom-forming macroalgae. *Mar. Pollut. Bull.* 56, 261–269. <https://doi.org/10.1016/j.marpolbul.2007.10.031>.
- Trodd, W., O'Boyle, S., 2021. *Water Quality in 2020. An Indicator Report*. EPA, Wexford (Ireland).
- Valiela, I., McClelland, J., Hauxwell, J., Behr, P.J., Hersh, D., Foreman, K., 1997. Macroalgal blooms in shallow estuaries: controls and ecophysiological and ecosystem consequences. *Limnol. Oceanogr.* 42, 1105–1118. <https://doi.org/10.4319/lo.1997.42.5.part.2.1105>.
- Vergara, J.J., Sebastian, M., Perez-llorens, J.L., Hernández, I., 1998. Photoacclimation of *Ulva rigida* and *U. rotundata* (Chlorophyta) arranged in canopies. *Mar. Ecol. Prog. Ser.* 165, 283–292.
- Viana, I.G., Bode, A., 2013. Stable nitrogen isotopes in coastal macroalgae: geographic and anthropogenic variability. *Sci. Total Environ.* 443, 887–895. <https://doi.org/10.1016/j.scitotenv.2012.11.065>.
- Viana, I.G., Bode, A., 2015. Variability in $\delta^{15}\text{N}$ of intertidal brown algae along a salinity gradient: differential impact of nitrogen sources. *Sci. Total Environ.* 512–513, 167–176. <https://doi.org/10.1016/j.scitotenv.2015.01.019>.
- Viana, I.G., Fernández, J.A., Aboal, J.R., Carballeira, A., 2011. Measurement of $\delta^{15}\text{N}$ in macroalgae stored in an environmental specimen bank for regional scale monitoring of eutrophication in coastal areas. *Ecol. Indic.* 11, 888–895. <https://doi.org/10.1016/j.ecolind.2010.12.004>.
- Villares, R., Carballeira, A., 2004. Nutrient limitation in macroalgae (*Ulva* and *Enteromorpha*) from the Rías Baixas (NW Spain). *Mar. Ecol.* 25, 225–243.
- Villares, R., Puente, X., Carballeira, A., 2001. *Ulva* and *Enteromorpha* as indicators of heavy metal pollution. *Hydrobiologia* 462, 221–232.
- Wan, A.H.L., Wilkes, R.J., Heesch, S., Bermejo, R., Johnson, M.P., Morrison, L., 2017. Assessment and characterisation of Ireland's green tides (*Ulva* species). *PLoS One* 12, e0169049. <https://doi.org/10.1371/journal.pone.0169049>.
- Wang, Ying, Wang, You, Zhu, L., Zhou, B., Tang, X., 2012. Comparative studies on the ecophysiological differences of two green tide macroalgae under controlled laboratory conditions. *PLoS One* 7. <https://doi.org/10.1371/journal.pone.0038245>.
- Wells, E., Wilkinson, M., Wood, P., Scanlan, C., 2007. The use of macroalgal species richness and composition on intertidal rocky seashores in the assessment of ecological quality under the European water framework directive. *Mar. Pollut. Bull.* 55, 151–161. <https://doi.org/10.1016/j.marpolbul.2006.08.031>.
- Wilkinson, M., Wood, P., Wells, E., Scanlan, C., 2007. Using attached macroalgae to assess ecological status of British estuaries for the European water framework directive. *Mar. Pollut. Bull.* 55, 136–150. <https://doi.org/10.1016/j.marpolbul.2006.09.004>.
- Worm, B., Lotze, H.K., Boström, C., Engkvist, R., Labanuskas, V., Sommer, U., 1999. Marine diversity shift linked to interactions among grazers, nutrients and propagule banks. *Mar. Ecol. Prog. Ser.* 185, 309–314.
- Yabe, T., Ishii, A.Y., Amano, A.Y., Koga, T., Hayashi, A.S., Nohara, A.S., 2009. Green tide formed by free-floating *Ulva* spp. at Yatsu tidal flat, Japan. *Limnology* 10, 239–245. <https://doi.org/10.1007/s10201-009-0278-4>.